

Resonances in $^{28}\text{Si}+^{28}\text{Si}$. I

— *Dinuclear Molecular Model with Axial Asymmetry* —

Eiji UEGAKI¹ and Yasuhisa ABE²

¹*Graduate School of Engineering and Resource Science, Akita University,
Tegata, Akita City 010-8502, Japan*

²*Research Center for Nuclear Physics, Osaka University,
10-1 Mihogaoka, Ibaraki, Osaka 567-0047, Japan*

A molecular model developed for resonances observed in medium light heavy-ion collisions is described. At high spins in $^{28}\text{Si} + ^{28}\text{Si}$ (oblate-oblate system), a stable dinuclear configuration is found to be equator-equator touching one. The normal modes around the equilibrium are investigated. These modes are expected to be the origin of a large number of resonances observed. Furthermore, due to the axially asymmetric shape of the stable configuration of $^{28}\text{Si} + ^{28}\text{Si}$, the system rotates preferentially around the axis with the largest moment of inertia, which gives rise to wobbling motion (K -mixing). Energy spectra for the normal modes and for the extended model including the wobbling motion are given.

Subject Index: 223

§1. Introduction

Intermediate resonances observed in heavy-ion scattering have offered intriguing subjects in nuclear physics. High-spin resonances well above the Coulomb barrier in the $^{24}\text{Mg} + ^{24}\text{Mg}$ and $^{28}\text{Si} + ^{28}\text{Si}$ systems exhibit very narrow widths, which suggest rather long lived compound nuclear states.^{1),2)}

Betts et al. firstly observed a series of resonance-like enhancements at $\theta_{\text{cm}} = 90^\circ$ in elastic scattering of $^{28}\text{Si} + ^{28}\text{Si}$, in the energy range from $E_{\text{lab}} = 101\text{MeV}$ to 128MeV with broad bumps of about 2MeV width. They gave spin assignments of $J = 34 \sim 42$ by the Legendre-fits to the elastic angular distributions for each bump, which correspond to the grazing partial waves.^{3),4)}

They further closely investigated angle-averaged excitation functions for the elastic and inelastic scattering in the energy region corresponding to $J = 36 - 40$, and found, in each bump, several sharp peaks correlating among the elastic and inelastic channels.^{5),6)} The total widths of those resonances are about 150keV , and the inelastic decay strengths are enhanced and stronger than the elastic one, which suggests that they are special eigenstates of the compound system. Similar sharp resonance peaks are observed by Zurmühle et al. in the $^{24}\text{Mg} + ^{24}\text{Mg}$ system.⁷⁾ The level densities observed in those systems are over one per MeV , which suggests activation of internal degrees of freedom, in addition to the radial motion. The decay widths of the elastic and inelastic channels up to high spin members of the ^{24}Mg or ^{28}Si ground rotational band exhaust about 30% of the total widths, whereas those into α -transfer channels are much smaller.^{8),9)} These enhancements of symmetric-mass decays strongly suggest dinuclear molecular configurations for the resonance states.

It is also noted that the widths of the elastic channel are rather small, for example, a few keV, being quite different from high spin resonances in lighter systems such as $^{12}\text{C} + ^{12}\text{C}$ and $^{16}\text{O} + ^{16}\text{O}$, which are well explained by the Band Crossing Model (BCM),¹⁰⁾ i.e., by couplings between the relative motion of the incident ions and the low-lying collective excitations of the ions.

From viewpoints of nuclear structure studies, one immediately thinks of secondary minima in fission of heavy nuclei, or of superdeformations which have been intensively studied in medium mass nuclei.¹¹⁾ Actually Bengtsson *et al.* made Nilsson-Strutinsky calculations for shape isomers of ^{56}Ni and obtained an energy minimum at large deformation, which appears to correspond to a dinuclear configuration.¹²⁾ Recently, a couple of microscopic calculations have been performed with expectation of existing shape-isomer bands.^{13), 14)} For the $^A\text{Mg} + ^A\text{Mg}$ system ($A = 24$ or 26) with very high spins, theoretical works were made to obtain stable configurations.^{15), 16)} All those models, however, are not able to reproduce the level density of the sharp resonances as well as the decay properties observed.

Taking into account the difference from resonances in lighter systems and the level density of the sharp resonances observed, we have proposed a new dinucleus-molecular model for the high spin resonances in the $^{24}\text{Mg} + ^{24}\text{Mg}$ and $^{28}\text{Si} + ^{28}\text{Si}$ systems,^{17), 18), 19)} in which two incident ions are supposed to form a united composite system. It rotates as a whole in space with the internal degrees of freedom originating from interaction of the deformed constituent ions. This is in contrast with the viewpoint of BCM.

Actually, we have already applied the model to the $^{24}\text{Mg} + ^{24}\text{Mg}$ system to obtain a stable dinucleus configuration, using the folding potential. Normal modes of motion around the stable minimum were solved with harmonic approximations, and several characteristic modes were obtained, such as butterfly one, etc., which are expected to be responsible to the observed sharp resonances. Decay properties of those resonance states were analyzed and strong enhancements to the mutual excitation channels are obtained in agreement with experiments for the $^{24}\text{Mg} + ^{24}\text{Mg}$ system.²⁰⁾

The same model has been applied to $^{28}\text{Si} + ^{28}\text{Si}$.¹⁹⁾ As is expected from the experience on $^{24}\text{Mg} + ^{24}\text{Mg}$, there are several intrinsic modes with excitation energy of a few MeV to several MeV. They, thus, are expected to correspond to the sharp resonance peaks within each bump of the grazing J . Therefore, the present model appears promising also for the sharp high spin resonances observed in $^{28}\text{Si} + ^{28}\text{Si}$.

Recently, a new development has been obtained, giving attention to the remarkable difference between the $^{24}\text{Mg} + ^{24}\text{Mg}$ and $^{28}\text{Si} + ^{28}\text{Si}$ systems. In the former, the stable configuration is pole-to-pole one due to the prolate deformation of ^{24}Mg , while in the latter, it is the equator-to-equator configuration due to the oblate deformation of ^{28}Si . Therefore, the former composite system is axially symmetric in the equilibrium, while the latter is triaxial. Then, in the latter, strong K -mixing is kinematically induced, and results in a wobbling motion.^{21), 22)} Hence we have extended our molecular model so as to include couplings between states with different K -quantum numbers (projection of the total angular momentum on the molecular z' -axis). As a result, we have obtained new low-lying states due to a triaxial shape

of the equilibrium configuration. In practice, we do not treat Coriolis terms in the hamiltonian explicitly, but we diagonalize the hamiltonian of the asymmetric rotator to obtain the rotational spectrum.

Since the two different kind of models, i.e., the dinuclear molecular model and the asymmetric rotator are used to obtain the results, it is necessary to clarify the relation between them. We have studied simple examples of dinuclear systems by using the molecular model, and have found that the molecular model hamiltonian reduces to that of the asymmetric rotator in the sticking limit.²³⁾

The present paper has the twofold aim. One is to describe the molecular normal-mode analyses^{19),20)} as the full paper, and the other is to describe the development newly obtained. As for the former, a brief reminder of the molecular model is given in §2, where we present the coordinate system and the model hamiltonian in the rotating molecular frame. In addition, in Appendix A, we take up simple examples of quantization, to compare the kinetic energy expression described by the angular momenta in the laboratory frame with that in the molecular frame, and to clarify the role of the Coriolis terms. There, the sticking-limit condition of sharing the total angular momentum between the orbital motion and the fragment spins is also derived. In §3, structures of the $^{28}\text{Si} + ^{28}\text{Si}$ system are investigated. We begin with inspecting the multi-dimensional energy surface and look for the equilibrium configuration of the system. In §3.2, harmonic approximation is adopted to solve normal modes around the equilibrium. Firstly, an energy spectrum with good K -quantum numbers will be given. The symmetries of the system and the practical expressions of the wave functions are described in Appendices B and C.

In order to present the new development, section 4 is devoted to the analyses for the dinuclear system with axial asymmetry, which gives rise to wobbling motions (K -mixing) in extremely high spins. After K -mixing, the K -states are recombined into new states. The sequence of energy levels obtained by the diagonalization of the asymmetric rotator hamiltonian is given. A simple analytic solution is also discussed. In §4.2, we take up simple examples of the molecular model hamiltonians and see how they reduce to the asymmetric rotator hamiltonians. As a summary, in §5, we discuss on the structures of the $^{28}\text{Si} - ^{28}\text{Si}$ molecule theoretically explored.

Those molecular states are expected to be the origin of a large number of resonances observed, and hence theoretical analyses have been made. The results are in good agreements with the experimental data,^{9),22)} which will be given in the succeeding paper, no. II.²⁴⁾

§2. Dinuclear molecular model of the oblate-oblate system

First, we briefly recapitulate the new molecular model for heavy-ion resonances. Definitions and derivations of the expressions are given in detail in Ref. 18), for the prolate-prolate system. We have already proposed a new description of interacting two oblate-deformed nuclei such as $^{28}\text{Si} + ^{28}\text{Si}$.^{19),20)} In §2.1, we extend our consideration to the coordinates of the system including axially-asymmetric deformed constituent nuclei, for later descriptions in §4. Subsections 2.2 and 2.3 are devoted for the descriptions of the kinetic energy and the nucleus-nucleus potential, respec-

tively, some expressions of which are already published in Ref. 19) and in a part of Ref. 20).

The total system is described in terms of rotation of the whole system in space and of internal motions of all the other degrees of freedom such as the orientations of the deformation axes of two nuclei relative to the rotating molecular axes. We anticipate that there exists a stable geometrical configuration, i.e., a minimum in the potential energy of the internal degrees of the system. Actually as explained later, each typical stable configuration appears by strong attractive nuclear interaction between tips of two deformed nuclei, for prolate or oblate deformations, respectively. Accordingly, motions of their pole orientations should be treated as vibrational degrees of freedom around the geometrical equilibrium configuration, which is quite different from the usual description using "channels" in the weak coupling picture with the orbital angular momentum and the spins of the interacting nuclei.

2.1. Coordinate systems

The total system to be solved consists of two deformed nuclei interacting with each other. We expect the axial symmetry of the constituent nuclei and their constant deformations, corresponding to the states of the $K = 0$ ground rotational band. We thus start with seven degrees of freedom illustrated in Fig. 1(a), that is, the relative vector $\mathbf{R} = (R, \theta_2, \theta_1)$ and the Euler angles of the interacting nuclei $(\tilde{\alpha}_1, \tilde{\beta}_1)$ and $(\tilde{\alpha}_2, \tilde{\beta}_2)$, where the deformations of the constituent nuclei are taken to be oblate for ^{28}Si nuclei.²⁵⁾ When the constituent nuclei contact and interact strongly with each other, their deformations in the ground state may change, i.e., additional deformations may be induced, such as those associated with the surface γ -vibrations or the static asymmetric ones.²⁶⁾ In that case, we have additional degrees of freedom, $\tilde{\gamma}_1$ and $\tilde{\gamma}_2$, by which the nuclei rotate around their intrinsic z -axes. (Those degrees of freedom are not illustrated in Fig. 1, for simplicity.) We define the rotating molecular axis z' of the whole system with the direction of the relative vector of two interacting nuclei, as is shown in Fig. 1(b). In the molecular model, the intrinsic axes of each deformed nucleus are referred to the molecular frame as usual. We introduce new Euler angles of the interacting nuclei in the molecular frame $(\alpha_1, \beta_1, \gamma_1)$ and $(\alpha_2, \beta_2, \gamma_2)$ as in Fig. 1(b), which are related to $(\tilde{\alpha}_i, \tilde{\beta}_i, \tilde{\gamma}_i)$ by

$$\Omega_i(\alpha_i, \beta_i, \gamma_i) = \Omega_M^{-1}(\theta_1, \theta_2) \Omega_i(\tilde{\alpha}_i, \tilde{\beta}_i, \tilde{\gamma}_i), \quad i = 1, 2, \quad (2.1)$$

where Ω 's denote Euler rotations with respective angles, with indications of the rotations for the each constituent nucleus no. 1 or no. 2 by i . To obtain the configuration of Fig. 1, it may be more useful to describe in terms of successive rotations as $\Omega_i(\tilde{\alpha}_i, \tilde{\beta}_i, \tilde{\gamma}_i) = \Omega'_i(\alpha_i, \beta_i, \gamma_i) \Omega_M(\theta_1, \theta_2)$, where the second rotations Ω'_i refer to the molecular axes, i.e., to be operated on the intrinsic axes which are parallel to the rotated molecular axes (x', y', z') . Correspondingly $\Omega_M(\theta_1, \theta_2)$ appears to be multiplied from the right-hand side in this case. Later, we introduce $\theta_3 = (\alpha_1 + \alpha_2)/2$ as the third Euler angle for the rotation of the total system. The axes x' and y' in Fig. 1(b) indicate the axes after the rotation $\Omega_M(\theta_1, \theta_2)$, while the molecular axes $x'(\theta_3)$ and $y'(\theta_3)$ indicate after the whole rotation $\Omega_M(\theta_1, \theta_2, \theta_3)$. Note that for the constituent nuclei with the axial symmetry, $\tilde{\gamma}_i$ are not necessary, and we put $\tilde{\gamma}_i = 0$.

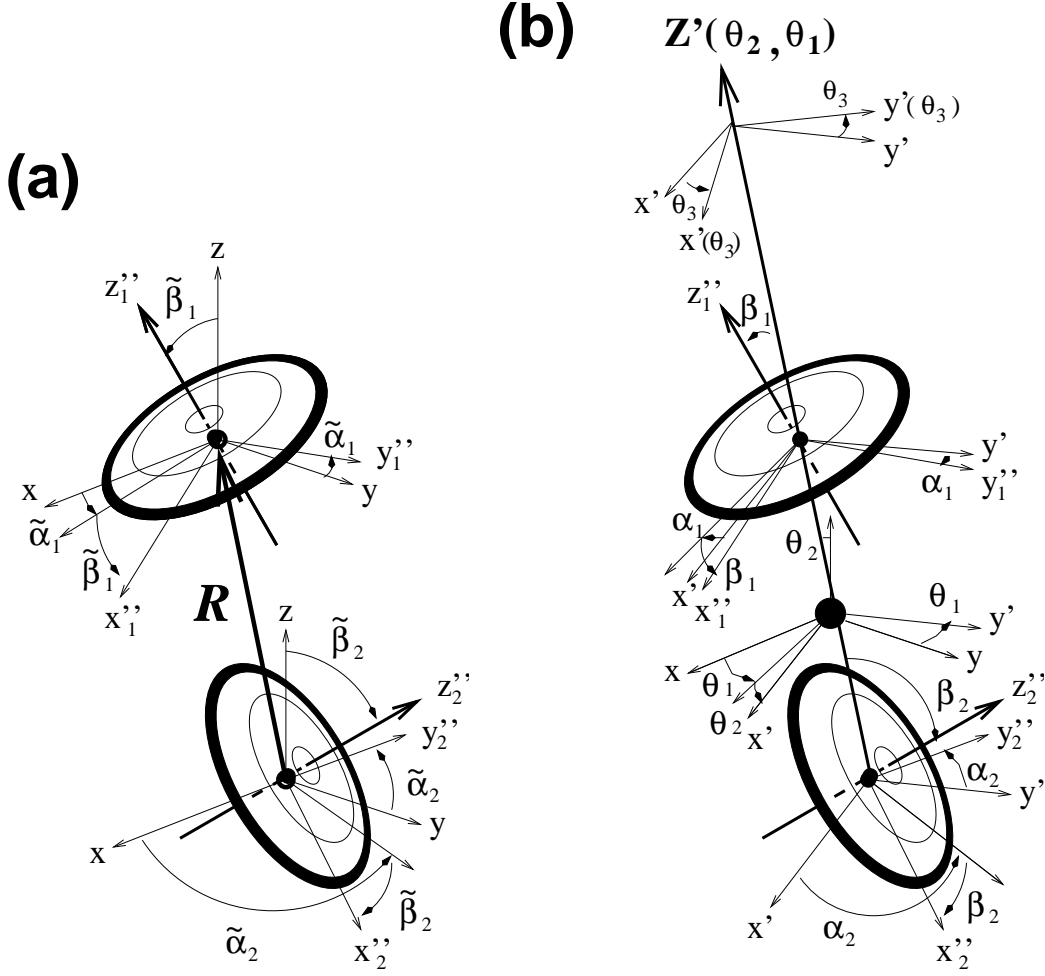


Fig. 1. The coordinates of an interacting dinuclear system. (a) shows the relative vector $\mathbf{R} = (R, \theta_2, \theta_1)$ and usual Euler angles $(\tilde{\alpha}_i, \tilde{\beta}_i)$ of the i -th nucleus referring to the laboratory frame. In (b), the molecular z' -axis and the seven degrees of freedom of the system are displayed, where the distance R is not indicated explicitly. The third angle θ_3 is defined by $\theta_3 = (\alpha_1 + \alpha_2)/2$ to give the whole rotation around the z' -axis.

Generally we obtain γ_i not to be zero due to the transformations between the coordinate systems, but these γ_i are physically meaningless. They appear in the rotational matrices, but they practically disappear in the inertia tensor of the total system; see Appendix B of Ref. 18).

Large deformations of the constituent nuclei may be induced in the deeply touching configurations of the resonances, then their axial symmetry of the deformations would be lost and the γ_i -degrees of freedom may appear. In the scope of the present model, we are able to introduce those degrees of freedom. However without information on the extent of the induced deformations nor on the dynamical properties about the deformations in the touching configurations, such efforts would bring no fruitful result. Later in §4.1, we consider configurations with such large induced

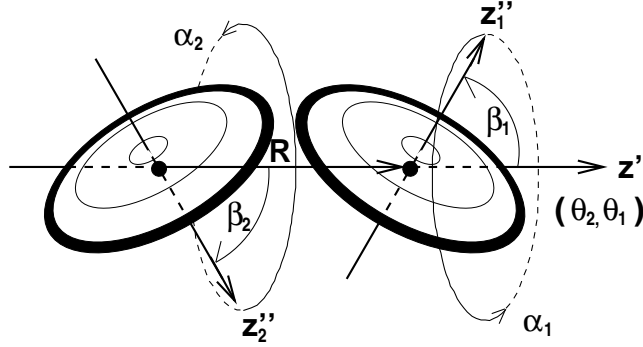


Fig. 2. The dinuclear configuration and the coordinates in the rotating molecular frame for an oblate-oblate system. The molecular z' -axis and the seven degrees of freedom of the system are displayed, where the α_1 - and α_2 -degrees are to be combined into $\theta_3 = (\alpha_1 + \alpha_2)/2$ and the degree of twisting $\alpha = (\alpha_1 - \alpha_2)/2$. The figure is the same as published in Refs. 19) and 20).

deformations, and investigate an example of the molecular model with the γ -degree of freedom in §4.2, but in this section we restrict ourselves to descriptions without induced deformations. This means that we assume the axial symmetry of the constituent nuclei with their moments of inertia $I_x = I_y$ and $I_z = 0$ in their principal axes, and that we start with the seven degrees of freedom as already mentioned. They are illustrated again in Fig. 2; the relative vector (R, θ_2, θ_1) and Euler angles of the interacting nuclei in the molecular frame (α_1, β_1) and (α_2, β_2) . The variables α_1 and α_2 are combined into variables $\theta_3 = (\alpha_1 + \alpha_2)/2$ and $\alpha = (\alpha_1 - \alpha_2)/2$. Then we have

$$(q_i) = (\theta_1, \theta_2, \theta_3, R, \alpha, \beta_1, \beta_2), \quad (2.2)$$

where θ_1, θ_2 and θ_3 are the Euler angles of the rotating molecular frame with the other four being internal variables.

2.2. Kinetic energy of the dinuclear molecule

Firstly we obtain an expression of the kinetic energy operator in terms of the above coordinates. We start with the classical kinetic energy of the system, which can be given in terms of the energies associated with the relative motion (the radial motion and the rotational motion of the two-ion centers) and the rotational motions of the two constituent nuclei,

$$T = \frac{1}{2}\mu\dot{R}^2 + \frac{1}{2}{}^t\boldsymbol{\omega}'\mathbf{I}_\mu(R)\boldsymbol{\omega}' + \frac{1}{2}{}^t\boldsymbol{\omega}_1\mathbf{I}_1\boldsymbol{\omega}_1 + \frac{1}{2}{}^t\boldsymbol{\omega}_2\mathbf{I}_2\boldsymbol{\omega}_2, \quad (2.3)$$

where R denotes the relative distance between the two-ion centers, μ being the reduced mass $m_1m_2/(m_1 + m_2)$ of the two nuclei with masses m_1 and m_2 , and the c.m. energy of the total system is omitted. The second term of the r.h.s. of Eq. (2.3) is the rotational energy of the two-ion centers given by the angular velocity of the molecular frame $\boldsymbol{\omega}'$ and the moment of inertia tensor $\mathbf{I}_\mu(R)$. The diagonal components I_{11} and I_{22} of the inertia tensor are μR^2 , the others being zero, which is associated with masses m_1 and m_2 at the relative distance R . Then the expression of the rotational energy is equal to usual one, $\frac{1}{2}\mu R^2(\dot{\theta}_2^2 + \dot{\theta}_1^2 \sin^2 \theta_2)$. The vectors $\boldsymbol{\omega}_1$

and $\boldsymbol{\omega}_2$ denote the angular velocities of the rotational motions of the two constituent nuclei, ${}^t\boldsymbol{\omega}_i$ being the transpose of $\boldsymbol{\omega}_i$. The inertia tensors of the two nuclei \mathbf{I}_1 and \mathbf{I}_2 are defined in the coordinate frames of their principal axes. Then, they are diagonal, elements of which are determined by the excitation energies of the members of the ground rotational bands of the constituent nuclei.

At this stage, the angular velocities of the constituent nuclei $\boldsymbol{\omega}_i$ in Eq. (2.3) are still those referred to the laboratory frame, so we have to express them in the molecular coordinate system, i.e., in terms of the angular velocity of the molecular frame $\boldsymbol{\omega}'$ and those $\boldsymbol{\omega}_i''$ referred to the molecular frame. Then we express the total kinetic energy as a sum of three parts, the total rotational energy T_{rot} associated with $\boldsymbol{\omega}'$, the internal kinetic energy T_{int} and the Coriolis coupling term T_C , as follows;

$$T = T_{\text{rot}} + T_{\text{int}} + T_C, \quad (2.4)$$

$$T_{\text{rot}} = \frac{1}{2} {}^t\boldsymbol{\omega}' \mathbf{I}_s \boldsymbol{\omega}', \quad (2.5)$$

$$T_{\text{int}} = \frac{1}{2} \mu \dot{R}^2 + \frac{1}{2} {}^t\boldsymbol{\omega}_1'' \mathbf{I}_1 \boldsymbol{\omega}_1'' + \frac{1}{2} {}^t\boldsymbol{\omega}_2'' \mathbf{I}_2 \boldsymbol{\omega}_2'', \quad (2.6)$$

$$T_C = {}^t\boldsymbol{\omega}' \{ {}^tR'(\alpha_1\beta_1\gamma_1) \mathbf{I}_1 \boldsymbol{\omega}_1'' + {}^tR'(\alpha_2\beta_2\gamma_2) \mathbf{I}_2 \boldsymbol{\omega}_2'' \}, \quad (2.7)$$

where $R'(\alpha_i\beta_i\gamma_i)$ denotes the transformation matrix (rotation matrix) which connects the axes of the molecular frame and the principal axes of each constituent nucleus. The total rotational energy T_{rot} is the rotational energy of the interacting constituent nuclei as a whole system, which rotates with the angular velocity $\boldsymbol{\omega}'$. The inertia tensor is given by

$$\mathbf{I}_s = \mathbf{I}_\mu(R) + {}^tR'(\alpha_1\beta_1\gamma_1) \mathbf{I}_1 R'(\alpha_1\beta_1\gamma_1) + {}^tR'(\alpha_2\beta_2\gamma_2) \mathbf{I}_2 R'(\alpha_2\beta_2\gamma_2), \quad (2.8)$$

where the first term of the r.h.s. denotes just the moments of inertia of two-ion centers, and the second and third terms are contributions from the constituent nuclei individually, though their "rotations" are already taken into account in Eq. (2.6). The internal kinetic energy T_{int} is those associated with the orientation degrees of freedom of the constituent nuclei in addition to the radial motion between them. The last two terms of the r.h.s. of Eq. (2.6) have a form of rotational energy, but their motions are not necessarily rotational. This is why the quotations are put on the word rotations above. Actually the nucleus-nucleus interaction favors cohesion of two constituent nuclei, which obstructs rotations of the constituent nuclei. Motions in the orientations are, therefore, not necessary to be rotational but would be rather confined, such as a sticking of the constituent nuclei and small fluctuations thereabout. In the sticking limit, the angular velocities $\boldsymbol{\omega}_i''$ are zero, while they are constant in free rotations. We, of course, anticipate intermediate states between the sticking limit and the rotation, i.e., fluctuations around the sticking configuration. For vibrational motions, for example, we consider fluctuations of the values of $\boldsymbol{\omega}_i''$ around zero, average values of them being to be zero.

After expressing those angular velocities with time derivatives of the corresponding Euler angles, we obtain a classical kinetic energy expression $\frac{1}{2} \sum g_{ij} \dot{q}_i \dot{q}_j$. And

then we quantize it by using the general formula for the curve-linear coordinate system,

$$\hat{T} = -\frac{\hbar^2}{2} \sum_{ij} \frac{1}{\sqrt{g}} \frac{\partial}{\partial q_i} \sqrt{g} (g^{-1})_{ij} \frac{\partial}{\partial q_j}, \quad (2.9)$$

where g and g^{-1} denote the determinant and the inverse matrix of (g_{ij}) , respectively. As the classical kinetic energy consists of the three parts, i.e., the total rotation, the internal motions and their couplings, the quantum mechanical operator for the kinetic energy \hat{T} is also given as a sum of three terms, $\hat{T} = \hat{T}_{\text{rot}} + \hat{T}_{\text{int}} + \hat{T}_{\text{C}}$. Naturally the term \hat{T}_{rot} is associated with the rotational variables $(\theta_1, \theta_2, \theta_3)$, \hat{T}_{int} with the internal variables $(R, \alpha, \beta_1, \beta_2)$ and \hat{T}_{C} with both. According to the derivation, \hat{T}_{rot} is expressed by the partial differential operators of θ_i . We combine those differential operators into angular momentum operators \hat{J}'_i referred to the molecular axes, as usual, i.e.,

$$\hat{T}_{\text{rot}} = \frac{\hbar^2}{2} \sum_{\substack{1 \leq i \leq 3 \\ 1 \leq j \leq 3}} \mu_{ij} \hat{J}'_i \hat{J}'_j, \quad (2.10)$$

where the matrix μ is the submatrix given later, and \hat{J}'_i 's are the angular momentum operators in terms of the Euler angles of the molecular frame,

$$\begin{aligned} \hat{J}'_1 &= -i \left(-\frac{\cos \theta_3}{\sin \theta_2} \frac{\partial}{\partial \theta_1} + \sin \theta_3 \frac{\partial}{\partial \theta_2} + \cot \theta_2 \cos \theta_3 \frac{\partial}{\partial \theta_3} \right), \\ \hat{J}'_2 &= -i \left(\frac{\sin \theta_3}{\sin \theta_2} \frac{\partial}{\partial \theta_1} + \cos \theta_3 \frac{\partial}{\partial \theta_2} - \cot \theta_2 \sin \theta_3 \frac{\partial}{\partial \theta_3} \right), \\ \hat{J}'_3 &= -i \frac{\partial}{\partial \theta_3}. \end{aligned} \quad (2.11)$$

Here Eq. (2.10) has a form just expected from the classical expression Eq. (2.5), but it should be noted that the submatrix μ is not exactly equal to the inverse of the inertia tensor \mathbf{I}_s , due to the Coriolis coupling. The coefficients μ_{ij} are given as follows, in terms of the internal variables $(R, \alpha, \beta_1, \beta_2)$,

$$\begin{aligned} \mu_{11} &= \mu_{22} = \frac{1}{\mu R^2}, \\ \mu_{12} &= 0, \\ \mu_{13} &= \frac{1}{2\mu R^2} \cos \alpha (\cot \beta_1 + \cot \beta_2), \\ \mu_{23} &= \frac{1}{2\mu R^2} \sin \alpha (\cot \beta_1 - \cot \beta_2), \\ \mu_{33} &= \frac{1}{4} \left[\left(\frac{1}{I_A} + \frac{1}{\mu R^2} \right) \frac{1}{\sin^2 \beta_1} + \left(\frac{1}{I_B} + \frac{1}{\mu R^2} \right) \frac{1}{\sin^2 \beta_2} \right] - \frac{1}{2\mu R^2} \\ &\quad + \frac{1}{2\mu R^2} \cos 2\alpha \cot \beta_1 \cot \beta_2, \end{aligned} \quad (2.12)$$

where I_A and I_B are the diagonal elements of the inertia tensors \mathbf{I}_1 and \mathbf{I}_2 , respectively. In the definition Eq. (2.11) of the total angular momentum operators \hat{J}'_i in

the body-fixed frame, we write them in terms of the Euler angles θ_i , which appear at the same time in the coordinates of the relative vector (R, θ, φ) between the two constituent nuclei, as $\theta = \theta_2$ and $\varphi = \theta_1$. Therefore the definition may be misleading as not to be the total angular momentum but to be the orbital angular momentum \mathbf{L} . In Appendix A, we take up simple examples of the quantization both in the laboratory frame and in the molecular frame, in order to see the relations between the coordinate sets and the definitions for the corresponding angular momentum operators. There, the role of the Coriolis coupling term is also clarified.

The internal kinetic energy operator is associated with the variables $(R, \alpha, \beta_1, \beta_2)$, as already mentioned. As usual, we introduce a volume element $dV = dR d\alpha d\beta_1 d\beta_2$ instead of the original $dV = D dR d\alpha d\beta_1 d\beta_2$ with $D = \mu^{3/2} R^2 I_A \sin \beta_1 I_B \sin \beta_2$, which means that the wave functions are defined with the additional factor \sqrt{D} . Accordingly we obtain

$$\hat{T}_{\text{int}} = \hat{O}_{\text{int}} + V_{\text{add}}, \quad (2.13)$$

$$\begin{aligned} \hat{O}_{\text{int}} = & -\frac{\hbar^2}{2} \left[\frac{1}{\mu} \frac{\partial^2}{\partial R^2} + \left(\frac{1}{I_A} + \frac{1}{\mu R^2} \right) \frac{\partial^2}{\partial \beta_1^2} + \left(\frac{1}{I_B} + \frac{1}{\mu R^2} \right) \frac{\partial^2}{\partial \beta_2^2} + \frac{2 \cos 2\alpha}{\mu R^2} \frac{\partial^2}{\partial \beta_1 \partial \beta_2} \right. \\ & + \frac{1}{4} \left\{ \left(\frac{1}{I_A} + \frac{1}{\mu R^2} \right) \frac{1}{\sin^2 \beta_1} + \left(\frac{1}{I_B} + \frac{1}{\mu R^2} \right) \frac{1}{\sin^2 \beta_2} - \frac{2}{\mu R^2} \right\} \frac{\partial^2}{\partial \alpha^2} \\ & - \frac{\partial}{\partial \alpha} \frac{\cos 2\alpha}{2\mu R^2} \cot \beta_1 \cot \beta_2 \frac{\partial}{\partial \alpha} \\ & \left. - \frac{1}{2\mu R^2} \left(\cot \beta_2 \frac{\partial}{\partial \beta_1} + \cot \beta_1 \frac{\partial}{\partial \beta_2} \right) \left(\sin 2\alpha \frac{\partial}{\partial \alpha} + \frac{\partial}{\partial \alpha} \sin 2\alpha \right) \right], \quad (2.14) \end{aligned}$$

$$\begin{aligned} V_{\text{add}} = & -\frac{\hbar^2}{8} \left[\left(\frac{1}{I_A} + \frac{1}{\mu R^2} \right) \left(\frac{1}{\sin^2 \beta_1} + 1 \right) + \left(\frac{1}{I_B} + \frac{1}{\mu R^2} \right) \left(\frac{1}{\sin^2 \beta_2} + 1 \right) \right. \\ & \left. + \frac{2 \cos 2\alpha}{\mu R^2} \cot \beta_1 \cot \beta_2 \right], \quad (2.15) \end{aligned}$$

where V_{add} is the term so-called additional potential due to the new volume element.

The Coriolis coupling operator \hat{T}_C consists of coupling operators between the variables $(\theta_1, \theta_2, \theta_3)$ and $(R, \alpha, \beta_1, \beta_2)$, i.e.,

$$\begin{aligned} \hat{T}_C = & \frac{\hbar^2}{\mu R^2} \left[i \sin \alpha \left(-\frac{\partial}{\partial \beta_1} + \frac{\partial}{\partial \beta_2} \right) \hat{J}'_1 + \cos \alpha \left(\frac{\partial}{\partial \beta_1} + \frac{\partial}{\partial \beta_2} \right) i \hat{J}'_2 \right. \\ & + \frac{i}{2} \sin 2\alpha \left(-\cot \beta_2 \frac{\partial}{\partial \beta_1} + \cot \beta_1 \frac{\partial}{\partial \beta_2} \right) \hat{J}'_3 \\ & - \frac{i}{4} (\cot \beta_1 - \cot \beta_2) \left(\frac{\partial}{\partial \alpha} \cos \alpha \hat{J}'_1 + \hat{J}'_1 \cos \alpha \frac{\partial}{\partial \alpha} \right) \\ & \left. - \frac{i}{4} (\cot \beta_1 + \cot \beta_2) \left(\frac{\partial}{\partial \alpha} \sin \alpha \hat{J}'_2 + \hat{J}'_2 \sin \alpha \frac{\partial}{\partial \alpha} \right) \right] \\ & + \frac{\hbar^2}{4} \left[\left(\frac{1}{I_A} + \frac{1}{\mu R^2} \right) \frac{1}{\sin^2 \beta_1} - \left(\frac{1}{I_B} + \frac{1}{\mu R^2} \right) \frac{1}{\sin^2 \beta_2} \right] \left(-i \frac{\partial}{\partial \alpha} \right) \hat{J}'_3, \quad (2.16) \end{aligned}$$

where the derivative operators of θ_i are again rewritten with the angular momentum operators \hat{J}'_i .

For details of some relations and explicit expressions, see Appendices of Ref. 18), for example, for the angular velocities in the molecular frame, the classical kinetic energy in terms of time derivatives of the Euler angles, their quantization and symmetries of the system.

In order to make the problem to be tractable, we start with good K -quantum numbers firstly, which is expected to be appropriate for the system of small axial asymmetry. For the $^{24}\text{Mg} + ^{24}\text{Mg}$ system (prolate-prolate one), for example, it is rather simple to intuitively understand, because stable configurations at high spins are dominantly elongated pole-pole ones which keep axial symmetry. However the $^{28}\text{Si} + ^{28}\text{Si}$ system (oblate-oblate one) favors equator-equator configurations, which do not have the axial symmetry intrinsically. So secondly, the effect of K -mixing is investigated later in §4.

At this stage, we therefore regroup the kinetic energy operator as follows,

$$\hat{T} = \hat{T}' + \hat{T}'_{\text{C}}, \quad (2.17)$$

$$\hat{T}' = \hat{T}'_{\text{rot}} + \hat{T}'_{\text{int}}, \quad (2.18)$$

where \hat{T}'_{C} includes the Coriolis coupling \hat{T}_{C} and the K -mixing terms in \hat{T}_{rot} . Accordingly the new rotational operator \hat{T}'_{rot} has good K -quantum numbers.

Let's restrict our discussion to *the rotation and vibration operator* \hat{T}' , together with the interaction potential given later. As the kinetic energy operator \hat{T}' keeps a good K -quantum number, eigenstates of the system are of a rotation-vibration type,

$$\Psi_{\lambda} \sim D_{MK}^J(\theta_i) \chi_K(R, \alpha, \beta_1, \beta_2). \quad (2.19)$$

Now the problem to be solved is of internal motions, i.e., motions associated with the internal variables $(R, \alpha, \beta_1, \beta_2)$ which couple with each other through the kinetic energy operator \hat{T}' and the interaction potential. For the later use in §3, we define the centrifugal potential given by \hat{T}'_{rot} with specified J and K ,

$$\begin{aligned} T'_{\text{rot}}(J, K) = & \frac{\hbar^2}{2} \left[\frac{1}{\mu R^2} \left\{ J(J+1) - \frac{3}{2} K^2 + \frac{1}{2} \cos 2\alpha \cot \beta_1 \cot \beta_2 (K^2 - 1) \right\} \right. \\ & \left. + \left(\frac{1}{I} + \frac{1}{\mu R^2} \right) \left(\frac{K^2 - 1}{4 \sin^2 \beta_1} + \frac{K^2 - 1}{4 \sin^2 \beta_2} - \frac{1}{2} \right) \right], \end{aligned} \quad (2.20)$$

where I denotes the moment of inertia of the constituent nuclei, i.e., $I = I_{\text{A}} = I_{\text{B}}$, since we are interested in the system of the identical constituent nuclei. In the expression of $T'_{\text{rot}}(J, K)$, we use the eigenvalue K instead of \hat{J}'_3 . Note that the additional potential V_{add} in Eq. (2.15) is moved into $T'_{\text{rot}}(J, K)$ for convenience, and similar terms of \hat{T}'_{rot} and V_{add} are amalgamated. In the numerical calculations, the value of I is estimated from the excitation energy of the 2_1^+ state of the ^{28}Si nucleus.

2.3. Nucleus-nucleus interaction potential

For the interaction potential, we want to have an expression that depends on geometrical configurations of interacting nuclei, i.e., a potential as a function of the Euler angles of the nuclei in addition to the radial distance between them. Proximity

potential appears to be one of the most suitable potentials,²⁷⁾ but it is rather laborious to calculate it for various configurations, i.e., one has to find out the shortest distance between two curved surfaces of arbitrarily-oriented deformed nuclei and to calculate curvatures etc. at the point. Instead, we employ a folding method. Since, in the double folding model, nuclear densities corresponding to geometrical molecular configurations are directly folded with effective nucleon-nucleon interactions, the model easily provides an interaction potential for the present purpose, i.e., as a function of the collective variables. As for the nucleon-nucleon interaction, we employ one that is called *density dependent* M3Y(DDM3Y),²⁸⁾

$$v(E, \rho, r) = f(E, \rho)g(E, r), \quad (2.21)$$

where $f(E, \rho)$ gives nucleon-density dependence by

$$f(E, \rho) = C(E)[1 + \alpha(E)e^{-\beta(E)\rho}], \quad (2.22)$$

ρ denoting density of nuclear matter in which the interacting nucleons are embedded, and $g(E, r)$ describes the original nucleon-nucleon interaction,

$$g(E, r) = \left[7999 \frac{e^{-4r}}{4r} - 2134 \frac{e^{-2.5r}}{2.5r} \right] + \hat{J}(E)\delta(\mathbf{r}). \quad (2.23)$$

The first term of $g(E, r)$ is M3Y potential without OPEP and the second term represents that from single-nucleon exchange, suggested by Satchler and Love.²⁹⁾ E is the bombarding energy per nucleon, which is chosen to be as suitable for the resonance energies ($E = 3.75\text{MeV}$ corresponding to $E_{\text{lab}} = 105\text{ MeV}$ for $^{28}\text{Si} + ^{28}\text{Si}$). At a short distance of the folding potential, i.e., with highly overlapping densities, DDM3Y gives weakly attractive potential. At the normal density, for example, the density-dependent factor $f(E, \rho)$ reduces the interaction strength by a factor about 3/4, compared with the original $g(E, r)$, while it is enhanced by a factor 1.2 at the half density, i.e., at the contact region.

The folding-model potential, however, is considered to be accurate only in the tail region of the nucleus-nucleus interaction. In the region where nuclear-density overlap goes beyond the normal density, it is considered to be not accurate enough. Hence, in addition to the folding potential with the nucleon-nucleon interaction, we introduce a phenomenological repulsive potential, which would originate from the effects of the Pauli principle among nucleons belonging to the interacting nuclei respectively, or from compression effects due to the overlapping density. We estimate strength of the repulsive potential due to the compression of nuclear density, from the equation of state of nuclear matter, i.e., from the binding energy as a function of nuclear density. One may think that the picture of the density overlap is doubtful in low energy, but the folding model does not take into account density redistribution, so it is consistent to account higher densities in the overlapping region. Anyhow, what we are interested in is the dynamics of two interacting nuclei in high spins where strong centrifugal forces dominate. Therefore, the long-range part of interactions is crucially important, but not the short-range part, which is treated more or less in a phenomenological way.

The folding potential is defined as usual,

$$U(\mathbf{R}) = \int d\mathbf{r}_1 \int d\mathbf{r}_2 \rho_1(\mathbf{r}_1) \rho_2(\mathbf{r}_2) v(\mathbf{r}_{12}),$$

$$\mathbf{r}_{12} = \mathbf{R} + \mathbf{r}_2 - \mathbf{r}_1, \quad (2.24)$$

where \mathbf{R} is the relative vector between the interacting nuclei and \mathbf{r}_i are referred to the centers of the nuclei, respectively. The long-range attractive part of the interaction potential in the molecular frame V_{attr} is obtained from $U(\mathbf{R})$ by taking the vector \mathbf{R} to be parallel to the z' -axis and by taking orientations of the density distributions of the constituent nuclei with respect to the molecular frame. By using Fourier transformation,

$$V_{\text{attr}} = \frac{1}{2\pi^2} \sum_{lm} i^{-l} Y_{lm}(\hat{\mathbf{R}}) \int dk k^2 j_l(kR) \int d\hat{\mathbf{k}} Y_{lm}^*(\hat{\mathbf{k}}) \tilde{v}(\mathbf{k}) \tilde{\rho}_1(\mathbf{k}) \tilde{\rho}_2(-\mathbf{k}), \quad (2.25)$$

$$\tilde{v}(\mathbf{k}) = \int d\mathbf{r} e^{i\mathbf{k}\mathbf{r}} v(r) = 4\pi \int dr r^2 j_0(kr) v(r), \quad (2.26)$$

$$\tilde{\rho}_i(\mathbf{k}) = \int d\mathbf{r}' e^{i\mathbf{k}\mathbf{r}'} \rho_i(\mathbf{r}'). \quad (2.27)$$

The density distribution $\rho_i(\mathbf{r}')$ in the molecular frame is related to that in the body-fixed frame, i.e., to that in the principal axes of the constituent nucleus; by Euler rotations, $\rho_i(\mathbf{r}') = \rho_i^B(\mathbf{r}_i'') = \hat{\mathcal{R}}(\alpha_i \beta_i \gamma_i) \rho_i^B(\mathbf{r}')$, where $\rho_i^B(\mathbf{r}_i'')$ is the density distribution in the principal axes and therefore

$$\rho_i^B(\mathbf{r}_i'') = \sum_{l=\text{even}} \rho_l(r_i'') Y_{l0}(\hat{\mathbf{r}}_i'') \quad (2.28)$$

with the assumed axial symmetry of each constituent nucleus. So the Fourier transform $\tilde{\rho}_i(\mathbf{k})$ is given with the Euler angles included as parameters,

$$\tilde{\rho}_i(\mathbf{k}) = \sum_l i^l \tilde{\rho}_l(k) \sum_{m'} D_{m'0}^{l*}(\alpha_i \beta_i \gamma_i) Y_{lm'}(\hat{\mathbf{k}}), \quad (2.29)$$

$$\tilde{\rho}_l(k) = 4\pi \int dr r^2 j_l(kr) \rho_l(r). \quad (2.30)$$

Inserting Eq. (2.29) with $i = 1$ and 2 into Eq. (2.25), we obtain the final form of the interaction potential as a function of the internal variables $(R, \alpha, \beta_1, \beta_2)$ in the following,

$$V_{\text{attr}}(R, \alpha, \beta_1, \beta_2) = \sum_{l'l''l} (2\pi)^{-3} i^{l'-l''-l} \hat{l}' \hat{l}'' (l' l'' 00 | l0)$$

$$\times F_{l'l''l}(R) G_{l'l''l}(\alpha, \beta_1, \beta_2),$$

$$F_{l'l''l}(R) = \int dk k^2 j_l(kR) \tilde{v}(k) \tilde{\rho}_{l'}(k) \tilde{\rho}_{l''}(k), \quad (2.31)$$

$$G_{l'l''l}(\alpha, \beta_1, \beta_2) = \sum_{m \geq 0} (-1)^m (2 - \delta_{m0}) (l' l'' m - m | l0)$$

$$\times \cos(2m\alpha) d_{m0}^{l'}(\beta_1) d_{m0}^{l''}(\beta_2).$$

It should be mentioned here that γ_i does not appear in the final expression due to the D -function with one magnetic quantum number being zero which originates from the axially-symmetric density distribution in Eq. (2·28), and that α_1 and α_2 are combined into $2\alpha = \alpha_1 - \alpha_2$ due to the fact that the vector \mathbf{R} is parallel to z' -axis, i.e., the magnetic quantum number associated with \mathbf{R} is zero. The Coulomb interaction is also folded, together with nuclear interaction $v(E, \rho, r)$ of Eq. (2·21).

We assume the density profile of $\rho_i^B(\mathbf{r}_i'')$ to be the Fermi distribution with $\rho_i^B(\mathbf{r}_i'') = \rho_0/[1 + \exp\{(r'' - R_N(\mathbf{r}_i''))/a_N\}]$, $R_N(\mathbf{r}_i'')$ denoting the radius of the deformed nucleus. As for the deformation of the constituent ^{28}Si nuclei, the existence of the hexadecapole deformation ($\beta_4 = 0.18 \pm 0.02$) is suggested from coupled-channel analyses for the elastic and inelastic neutron scattering.³⁰⁾ Therefore, we take the radius of each nucleus as $R_N(\mathbf{r}_i'') = r_0 A_i^{1/3} [1 + \beta_Q Y_{20}(\hat{\mathbf{r}}_i'') + \beta_H Y_{40}(\hat{\mathbf{r}}_i'')]$ including two parameters β_Q and β_H for the deformations, the values of which are determined to be -0.46 and 0.22 , respectively, according to the suggested value for the ratio β_Q/β_H and their magnitudes adjusted with the $B(E2)$ value of the ground-rotational band of ^{28}Si .³¹⁾ The value of r_0 is taken to be 1.03fm from the textbook of Bohr-Mottelson,³²⁾ and a_N to be 0.48fm to reproduce the RMS radius of the ground state.

Next, we proceed to *the effect of density overlap* in the inner region, where the folding potential is not expected to be adequate. An overlapping of the densities brings about a higher nuclear density than the normal one, which gives rise to a binding energy loss of the interacting system in addition to the attractive folding potential. We take into account the effect as a repulsive potential to be added to the folding one given in Eq. (2·24). The volume with higher density depends on the configurations of the constituent nuclei, especially on their relative distance. Actually, the overlapping of two nuclei produces nuclear density from zero to twice of the normal density. An accurate calculation of the effect, therefore, is rather laborious. We propose a simple approximate way. If we assume the density profile to be of sharp cut-off or with a very small diffuseness, an overlapping volume has always twice of the normal density. So the short-range repulsive effect is expected to be proportional to the overlapping volume, and it would be simulated by a potential

$$V_{\text{rep}}(R, \alpha, \beta_1, \beta_2) = V_P \int \delta(r_{12}) \rho_1'(\mathbf{r}_1) \rho_2'(\mathbf{r}_2) d\mathbf{r}_1 d\mathbf{r}_2, \quad (2\cdot32)$$

where the primes on the densities indicate Fermi distributions with a small diffuseness a_P . The strength V_P of V_{rep} is chosen in the following, referring to the Equation of State (EOS) of nuclear matter. Thus the total interaction potential is given by

$$V_{\text{int}} = V_{\text{attr}} + V_{\text{rep}}, \quad (2\cdot33)$$

where V_{attr} denotes the usual folding potential defined in Eq. (2·24). The repulsive potential looks like a folding potential of the zero-range interaction, but has the primed densities instead of the normal density distributions. Of course, we can utilize a merit of the form of Eq. (2·32) in the actual calculations.

To determine the strength V_P , we use EOS of the nuclear matter, i.e., a binding energy loss per nucleon $\Delta\varepsilon$ for twice of the normal density which is calculated under

the condition of complete overlap at the $R = 0$ limit. Without Coulomb energy the value of $\Delta\varepsilon$ can be taken to be $7 \sim 11\text{MeV}$ ³³⁾ from the values of the nuclear compression modulus $K_\infty = 180 \sim 240\text{MeV}$,³⁴⁾ which is suggested by the experiments on giant monopole resonances. Hence the values $a_P = 0.25\text{fm}$ and $V_P = 330\text{MeVfm}^3$ are obtained to reproduce $\Delta\varepsilon = 9\text{MeV}$ in the $^{28}\text{Si} + ^{28}\text{Si}$ system. Radial forms of the folding potential are shown in Fig. 3, for the stable geometrical configurations (parallel equator-equator ones, see the next section), where the effective potentials for $J = 0$ and $J = 38$ are displayed. Details of the folding potentials about their dependences on a_P and V_P are already discussed in Ref. 20), where the effects of hexadecapole deformation in ^{28}Si nuclei are also investigated.

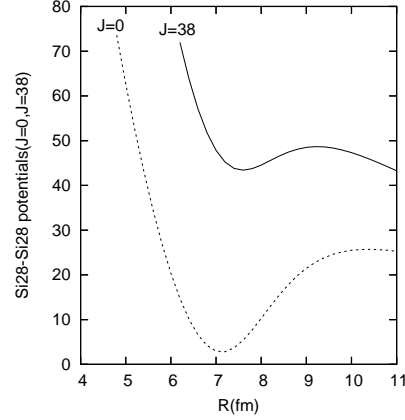


Fig. 3. The radial forms of the effective potentials in the parallel equator-equator configuration of $^{28}\text{Si} + ^{28}\text{Si}$, $V_{JK}(R) = V_{\text{int}}(R, \pi/2, \pi/2, \pi/2) + T'_{\text{rot}}(J, K)$ for spins $J = 0$ and $J = 38$ with $K = 0$ are shown.

§3. Dinuclear structures of the $^{28}\text{Si} + ^{28}\text{Si}$ system

3.1. Stable configuration of the oblate-oblate system with high spins

In order to know dynamical aspects of multi-dimensional internal motion, we calculate the effective potential with specified spin J and K , defined as follows:

$$V_{JK}(R, \alpha, \beta_1, \beta_2) = V_{\text{int}}(R, \alpha, \beta_1, \beta_2) + T'_{\text{rot}}(J, K). \quad (3.1)$$

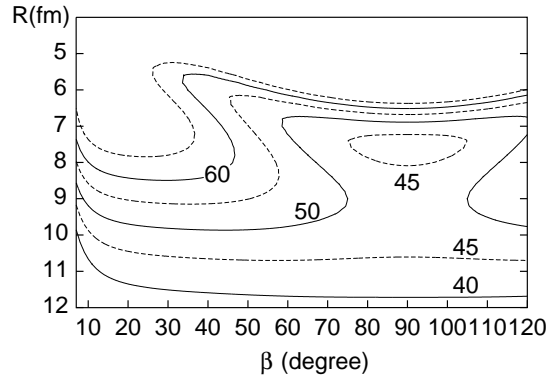


Fig. 4. The effective potential energy V_{JK} for the $^{28}\text{Si} + ^{28}\text{Si}$ system with $J = 38$ and $K = 0$ is displayed, for the $R - \beta(\beta_1 = \beta_2)$ degrees at $\alpha = \pi/2$. A local energy minimum exists at $R = 7.6\text{fm}$. Contours are in MeV. The figure is essentially the same as the energy contour map in Refs. 19) and 20).

In Fig. 4, an $R - \beta(\beta_1 = \beta_2)$ energy surface, i.e., $V_{JK}(R, \pi/2, \beta, \beta)$ is displayed for $J = 38$ and $K = 0$. We find a local minimum point at $\beta_1 = \beta_2 = \pi/2$ and $R = 7.6\text{fm}$, namely, at the equator-equator(E-E) configuration, with a rather deep potential well around the equilibrium. We mention that the some expressions, numerical results and figures in this section are already published in Refs. 19) and 20), but we show them for explanation.

In Fig. 5(a), the α -dependence of V_{JK} in the E-E configuration at the equilibrium distance is shown. (Note that our definition for the domain of the variables is $0 \leq \alpha < \pi$ and $0 \leq \beta_1, \beta_2 \leq \pi$.) We find that the α -dependence is extremely weak. Another point is that we have two local minima at $\alpha = 0$ and $\pi/2$. Those two configurations are, however, exactly the same, namely, *parallel* E-E configuration (z'' -axes of the constituent nuclei are parallel). Therefore it is necessary to impose symmetry on the wave functions. In Fig. 5(b), β -dependences of V_{JK} with $\beta_1 = \beta_2$ are compared between at $\alpha = 0$ and at $\alpha = \pi/2$, where solid line is for $\alpha = \pi/2$ (the cross section of Fig. 4 at $R = R_e = 7.6\text{fm}$) and dashed line for $\alpha = 0$. (Note that configurations with $\beta_1 = \beta_2 \neq \pi/2$ at $\alpha = 0$ are not the same as those with the same

β_i -values at $\alpha = \pi/2$, but are the same as those with $\beta_1 = \pi - \beta_2$ at $\alpha = \pi/2$.) The β -well at $\alpha = \pi/2$ is seen to be rather shallow, compared with that at $\alpha = 0$. Hence, despite the weak α -dependence of V_{JK} in the E-E configuration, we have significantly α -dependent restoring force for β -motions around the E-E configuration.

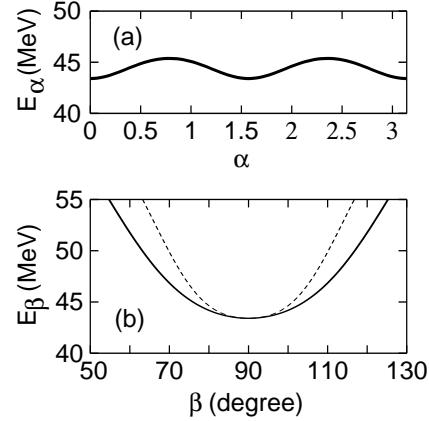


Fig. 5. (a) the α -dependence of the effective potential V_{JK} with $J = 38$ and $K = 0$, for the E-E configuration at $R = R_e = 7.6\text{fm}$. (b) V_{JK} versus $\beta = \beta_1 = \beta_2$ at $\alpha = 0$ and at $\alpha = \pi/2$, which are displayed by dashed and solid lines, respectively. The figure is the same as published in Refs. 19) and 20).

3.2. Harmonic approximation and normal modes with a specified K

In order to solve normal modes for four variables ($R, \alpha, \beta_1, \beta_2$), we expand V_{JK} into a quadratic form for R, β_1 and β_2 , at the equilibrium E-E configuration, while for α we keep its dependence exactly in terms of $\cos(2m\alpha)$ series, such as those given in the interaction potential of Eq. (2.31). Then the effective potential is expressed as

$$\begin{aligned}
 V_{JK}(R, \alpha, \beta_1, \beta_2) = & V_{JK}(R_e, \alpha, \frac{\pi}{2}, \frac{\pi}{2}) + \frac{k_R}{2}(R - R_e)^2 \\
 & + \frac{1}{2}k_\beta^{11}(\alpha)\Delta\beta_1^2 + \frac{1}{2}k_\beta^{22}(\alpha)\Delta\beta_2^2 \\
 & + k_\beta^{12}(\alpha)\Delta\beta_1\Delta\beta_2 + (\text{higher order}), \quad (3.2)
 \end{aligned}$$

where $\Delta\beta_i$ denotes $\beta_i - \pi/2$. $k_\beta^{ij}(\alpha)$ denotes the second derivative $\partial^2 V_{JK}/\partial\beta_i\partial\beta_j$, $k_\beta^{11}(\alpha)$ being equal to $k_\beta^{22}(\alpha)$. Although $k_\beta^{ij}(\alpha)$ is a coefficient of $\Delta\beta_i\Delta\beta_j$ in the expansion, it is a function of α , i.e., we take into account α -dependence of the coefficient, in addition to the α -dependence of $V_{JK}(R_e, \alpha, \frac{\pi}{2}, \frac{\pi}{2})$. As $k_\beta^{11}(\alpha)$ consists of $\cos(2m\alpha)$ series with $m = \text{even}$ including zero, the major part is a constant k_0 from $m = 0$. We write $k_\beta^{11}(\alpha) = k_\beta^{22}(\alpha) = k_0 + k_2(\alpha)$, $k_2(\alpha)$ being a sum of contributions from terms with $m = \text{even} > 0$.

We introduce new coordinates in order to eliminate cross products of β_1 and β_2 both in \hat{T}_{int} and in the quadratic expansion of V_{JK} . The new variables describe *butterfly* and *anti-butterfly* modes as follows:

$$\begin{aligned}\beta_+ &= (\Delta\beta_1 + \Delta\beta_2)/\sqrt{2} = (\beta_1 + \beta_2 - \pi)/\sqrt{2}, \\ \beta_- &= (\Delta\beta_1 - \Delta\beta_2)/\sqrt{2} = (\beta_1 - \beta_2)/\sqrt{2}.\end{aligned}\quad (3.3)$$

Furthermore the inertia masses of three variables α, β_+ and β_- are approximated by the values given at the E-E configuration. Combining the kinetic energy operator and the expanded effective potential, the total hamiltonian is given as follows:

$$H = H_0 + T'_C + (\text{higher order}), \quad (3.4)$$

$$H_0 = H_R + H_{\text{angl}}(\beta_+, \beta_-, \alpha), \quad (3.5)$$

$$H_R = -\frac{\hbar^2}{2\mu} \frac{\partial^2}{\partial R^2} + \frac{k_R}{2}(R - R_e)^2, \quad (3.6)$$

$$\begin{aligned}H_{\text{angl}}(\beta_+, \beta_-, \alpha) &= H_+(\beta_+, \alpha) + H_-(\beta_-, \alpha) \\ &\quad - \frac{\hbar^2}{4I} \frac{\partial^2}{\partial \alpha^2} + V_{JK}(R_e, \alpha, \frac{\pi}{2}, \frac{\pi}{2}),\end{aligned}\quad (3.7)$$

$$H_\pm(\beta_\pm, \alpha) = -\frac{\hbar^2}{2} \left(\frac{1}{I} + \frac{1 \pm \cos 2\alpha}{\mu R_e^2} \right) \frac{\partial^2}{\partial \beta_\pm^2} + \frac{k_\pm(\alpha)}{2} \beta_\pm^2, \quad (3.8)$$

where $+$ or $-$ sign of \pm in Eq. (3.8) corresponds to the β_+ and β_- degrees of freedom, respectively, with $k_+(\alpha) = k_0 + k_2(\alpha) + k_\beta^{12}(\alpha)$ and $k_-(\alpha) = k_0 + k_2(\alpha) - k_\beta^{12}(\alpha)$.

Now we solve the Schrödinger equation with the hamiltonian H_0 for the internal four degrees of freedom, which is separated into two parts. One is the hamiltonian H_R for the radial motion and nothing but that of a simple one dimensional harmonic oscillator. Another is H_{angl} for the angle variables α, β_+ and β_- , which is also *almost separable* into H_+ of β_+ , H_- of β_- and the remaining hamiltonian for α . H_+ and H_- again represent harmonic oscillators, although the masses and the restoring forces depend on α . Hence we analytically obtain wave functions for H_\pm and their energy quanta $\hbar\omega_\pm$ with the frequencies

$$\omega_\pm = \sqrt{k_\pm(\alpha) \left(\frac{1}{I} + \frac{1 \pm \cos 2\alpha}{\mu R_e^2} \right)}. \quad (3.9)$$

Taking into account those vibrational energies from the β -degrees of freedom, we introduce a reduced potential for the α -motion, and obtain the Schrödinger equation for the α -motion as follows:

$$\left[-\frac{\hbar^2}{4I} \frac{\partial^2}{\partial \alpha^2} + V_{JK}(R_e, \alpha, \frac{\pi}{2}, \frac{\pi}{2}) + E_{n_+, n_-}^\beta(\alpha) \right] \phi(\alpha) = E_{\text{angl}} \phi(\alpha), \quad (3.10)$$

where $E_{n_+, n_-}^\beta(\alpha)$ denotes vibrational energy $(n_+ + 1/2)\hbar\omega_+ + (n_- + 1/2)\hbar\omega_-$ from $H_+ + H_-$, added as a part of the reduced potential. Note that, in order to obtain analytic form of $\hbar\omega_\pm$ in $\cos(2m\alpha)$ series, we expand square root in Eq. (3.9) supposing $\omega_0 = \sqrt{k_0(1/I + 1/\mu R_e^2)}$ to be the leading term. Accordingly, we consider a solution $\phi(\alpha)$ of Eq. (3.10) to be described by cosine and sine functions of α , i.e., Fourier series, as the reduced potential $V_{JK}(R_e, \alpha, \frac{\pi}{2}, \frac{\pi}{2}) + E_{n_+, n_-}^\beta(\alpha)$ is described by a sum of $\cos(2m\alpha)$. Then Eq. (3.10) is reduced to a secular equation, which is easily solved. Thus the eigenenergy of the system is given as follows, specified by the quantum numbers $(n, n_+, n_-, K, (\nu, \pi_\alpha))$,

$$\begin{aligned} E^J(n, n_+, n_-, K, (\nu, \pi_\alpha)) = & E_0(R_e) + \frac{\hbar^2}{2} \left[\frac{J(J+1) - K^2 - 1}{\mu R_e^2} + \frac{K^2 - 2}{2I} \right] \\ & + \left(n + \frac{1}{2} \right) \hbar\omega_R \\ & + (n_+ + n_- + 1) \hbar\omega_0 + E_\nu^\alpha(\pi_\alpha), \end{aligned} \quad (3.11)$$

where ν denotes a dominant frequency of the α -motion with π_α for the parity concerning the reflection at the equilibrium of $\alpha = \pi/2$. The first and second terms in the r.h.s. of Eq. (3.11) are constant energies from the interaction potential and the centrifugal energy included in V_{JK} at the equilibrium, respectively. $(n_+ + n_- + 1)\hbar\omega_0$ and $E_\nu^\alpha(\pi_\alpha)$ are the vibrational energies for the β -motions without the α -dependence and the energy for the α -motion, respectively.

There is a selection rule $K \pm \nu = \text{even}$ for the α -motion. Because of the parity and boson symmetries, n_+ can be taken to be larger than or equal to n_- . For the β -vibrational modes, we have a rule $(-1)^{n_+ + n_-} = (-1)^K$ due to the symmetry of each constituent nucleus under the space inversion. Details of the symmetries of the molecular system, the wave functions and the selection rule are given in Appendix B. The resultant states are summarized in Table I. Note that the eigenfunction of the α -motion is not necessarily the internal rotation specified with a single ν -value, and that mixing over allowed ν -states is expected.

Table I. Molecular states allowed by the selection rule, specified by the K -quantum number, the β -vibrational quanta (n_+, n_-) and ν for the α -motion.

K	(n_+, n_-)	ν
0	(0,0), (2,2)	0, 4, 8, ...
0	(2,0), (4,0), (4,2)	0, 2, 4, 6, ...
2	(0,0), (1,1), (2,2)	2, 6, 10, ...
4	(0,0), (1,1), (2,2)	0, 4, 8, ...
2, 4	(2,0), (4,0), (4,2)	0, 2, 4, 6, ...
1, 3	(1,0), (2,1)	1, 3, 5, ...

In Fig. 6, molecular normal modes of $^{28}\text{Si} + ^{28}\text{Si}$ with spin 38 are displayed, classified with the K -quantum numbers. The twisting-mode excitations associated

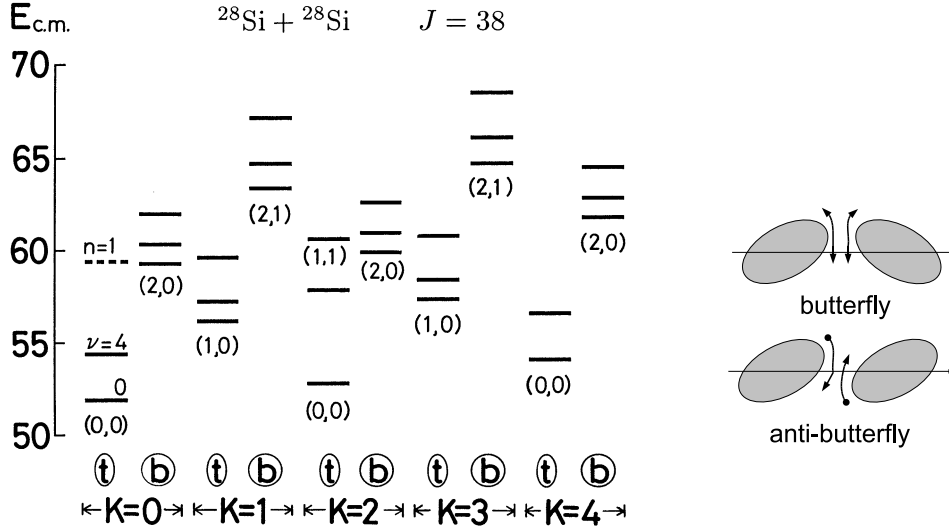


Fig. 6. Molecular normal modes for the $^{28}\text{Si} + ^{28}\text{Si}$ system for $J = 38$. The quantum states are specified by $(n, n_+, n_-, K, (\nu, \pi_\alpha))$, where $n = 0$ is given except for one level ($n = 1, \nu \sim 0$) displayed with dashed line. The quanta (n_+, n_-) of the β -motions are given below the levels, and K at the bottom. (t) and (b) marks assigned in the lower part of the figure indicate the twisting rotational mode and the butterfly modes, respectively. Also given above some levels with $K = 0$ are dominant values of the quantum number ν for the α -motion. On the right-hand side, butterfly and anti-butterfly motions are illustrated. The figure on the l.h.s. is the same as published in Refs. 19) and 20).

with the α -degree are obtained, and indicated by marked (t) at the bottom. Also given above each level with $K = 0$ and (t) is the dominant quantum number of ν for the α -motion, which means the α -motion is approximately described by a single term $\cos \nu\alpha$. The butterfly and anti-butterfly vibrational modes are indicated by marked (b). A pair of quanta (n_+, n_-) is given below the levels. All those are due to the internal degrees of freedom, i.e., intrinsic excitations. Apparently the K -excitation and the twisting rotational mode appear to be lower than the β -vibrational modes. The excitation energy for $K = 2$ is very small, smaller than 1 MeV, and even those for $K = 4$ or $\nu = 4$ are smaller than 3 MeV.

In Fig. 7(a), a few examples of wave functions for the α -motion are exhibited, where the β -modes are in the zero-point oscillation (dashed line) or the 2-quanta excitation of butterfly (solid line). We see that, with zero quanta for the β -modes, the amplitude is wriggling around the value of the unit, the equilibria $\alpha = 0$ and $\pi/2$ being slightly favored. (With exact $\nu = 0$ we have a constant behavior. Weak $\nu = 4$ mixing exists.) With 2 quanta for the butterfly mode, however, we find surprisingly strong concentration around the equilibrium of $\alpha = \pi/2$. In Fig. 7(b), we inspect the reduced α -potential for quanta (2, 0). Compared with the potential for (0, 0), we find that the minimum at $\alpha = 0$ disappears, and the potential well at $\alpha = \pi/2$ is extended to wider region, which sustains the localization of the amplitude. One

may wonder why the difference between $\alpha = 0$ and $\pi/2$ exists. The reason is as follows: at $\alpha = 0$, due to the definition of β_{\pm} , β -motion with $(n_+, n_-) = (2, 0)$ does not imply butterfly excitation but anti-butterfly one with 2 quanta. Such a characteristic of the β_{\pm} coordinates gives larger excitation energy for $(2, 0)$ at $\alpha = 0$ than at $\alpha = \pi/2$. In Fig. 7(c), the energy quanta $\hbar\omega_{\pm}$ versus α are shown, where we are able to confirm the point. Returning back to the dinuclear configuration, for a configuration with $\beta_1 = \beta_2 < \pi/2$, for example, we obtain a butterfly one at $\alpha = \pi/2$, such as displayed in Fig. 2, while at $\alpha = 0$ we obtain an anti-butterfly one with the same values of β_i . Hence the localization around $\alpha = \pi/2$, seen in Fig. 7(a), indicates nothing but a realization of a physical butterfly excitation. Thus, we are able to classify the levels in Fig. 6 into two groups, i.e., the twisting mode and the butterfly (or anti-butterfly) mode, respectively. Some examples of the wave functions for the normal modes are explicitly given in Appendix C.

§4. Rotational motion at extremely high spins with triaxial deformation

One of the characteristic features of the spectrum obtained theoretically is a series of low-energy K -rotational excitation due to axial asymmetry around molecular z -axis, which is in contrast with the $^{24}\text{Mg} + ^{24}\text{Mg}$ case.^{17), 18)} One can understand the reason immediately from Fig. 8, where the upper configuration ($^{24}\text{Mg} + ^{24}\text{Mg}$) has axial symmetry as a total system, but the lower one for $^{28}\text{Si} + ^{28}\text{Si}$ has axial asymmetry. Thus K is not a good quantum number, namely, we expect the eigenstates are K -mixed.

A triaxial system preferentially ro-

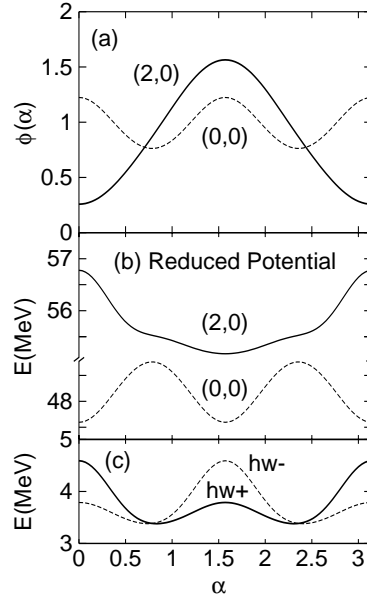


Fig. 7. (a) Wave functions for the α -motion for $J = 38$ and $K = 0$. Those with the zero-point oscillation $(0, 0)$ and the butterfly excitation $(2, 0)$ for the β -degrees of freedom are displayed, respectively. (b) The reduced α -potential $V_{JK}(R_e, \alpha, \pi/2, \pi/2) + E_{n_+, n_-}^\beta(\alpha)$. (c) α -dependences of the β -energy quanta $\hbar\omega_{\pm}$. The figure is the same as published in Refs. 19) and 20).

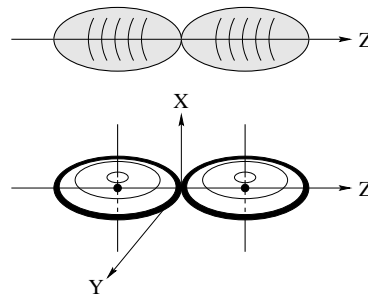


Fig. 8. Equilibrium configurations of two dinuclear systems. The upper portion is for $^{24}\text{Mg} - ^{24}\text{Mg}$ and the lower one for $^{28}\text{Si} - ^{28}\text{Si}$.

tates around the axis with the largest moment of inertia. By the definition of the axes in the lower panel of Fig. 8, we have the moments of inertia as $I_X > I_Y \gg I_Z$, due to the nuclear shape. Thus the system, which is seen as two pancake-like objects(^{28}Si 's) touching side-by-side, rotates around X -axis normal to the reaction plane. Such a motion is called as wobbling.

We extend our molecular model so as to include couplings between states with different K -quantum numbers. As a result, we will obtain new low-lying states due to the triaxial shape of the equilibrium configuration. The Coriolis terms in the molecular hamiltonian bring those couplings. However, in practice, we do not treat the Coriolis terms explicitly, but we diagonalize the hamiltonian of the asymmetric rotator to obtain the rotational spectrum.

The Coriolis terms in the molecular hamiltonian in Eq. (2.16) gives an impression that those are quite different from the asymmetric rotator. So the effect of the Coriolis coupling terms will be examined later in §4.2, to show that the molecular hamiltonian reduces to the asymmetric rotator hamiltonian in the sticking limit.

4.1. Analyses by asymmetric rotator

We describe the rotational motions of two pancake-like objects(^{28}Si 's) touching side-by-side by means of the asymmetric rotator. Generally its hamiltonian is written as follows, with the moments of inertia about the intrinsic axes I_x , I_y , and I_z , respectively;

$$\hat{T}_{\text{rot}} = \frac{\hbar^2}{2} \left(\frac{\hat{J}_x^2}{I_x} + \frac{\hat{J}_y^2}{I_y} + \frac{\hat{J}_z^2}{I_z} \right) \quad (4.1)$$

$$= \frac{\hbar^2}{2} \left\{ \frac{\hat{J}^2}{I_{\text{av}}} + \frac{1}{\Delta} (-\hat{J}_x^2 + \hat{J}_y^2) + \frac{1}{I_K} \hat{J}_z^2 \right\}, \quad (4.2)$$

where \hat{J}_x , \hat{J}_y and \hat{J}_z denote the components of the angular momentum operator along the intrinsic axes of the body-fixed frame (the same operators as defined in Eq. (2.11)). I_{av} , Δ and I_K in Eq. (4.2) are related to I_x , I_y and I_z by

$$\frac{1}{I_{\text{av}}} = \frac{1}{2} \left(\frac{1}{I_x} + \frac{1}{I_y} \right), \quad (4.3)$$

$$\frac{1}{\Delta} = -\frac{1}{I_x} + \frac{1}{I_{\text{av}}} = \frac{1}{I_y} - \frac{1}{I_{\text{av}}}, \quad (4.4)$$

$$\frac{1}{I_K} = \frac{1}{I_z} - \frac{1}{I_{\text{av}}}. \quad (4.5)$$

By using lowering and raising operators, \hat{J}_+ and \hat{J}_- of the angular momentum in the body-fixed frame, we obtain

$$\hat{T}_{\text{rot}} = \frac{\hbar^2}{2} \left\{ \frac{\hat{J}^2}{I_{\text{av}}} + \frac{\hat{J}_z^2}{I_K} - \frac{1}{2\Delta} (\hat{J}_+^2 + \hat{J}_-^2) \right\}, \quad (4.6)$$

where $\hat{J}_{\pm} \equiv \hat{J}_x \pm i\hat{J}_y$, respectively, which give rise to couplings between different K 's. The coupling strength is given by the coefficient $1/\Delta$, which is proportional to the

difference between $1/I_y$ and $1/I_x$. In an intuitive understanding, the rotation around x -axis is lower in energy than the rotation around y -axis due to $I_x > I_y$. When the energy difference between the rotations around the molecular x - and y -axes is larger than K -excitation energies, the K -mixing is expected to be rather large. In other words, an energetically favored motion, i.e., rotation around x -axis would be realized by the K -mixing.

In order to obtain an accurate description of this triaxial rotator, as it is well known for polyatomic molecules, we diagonalize the hamiltonian with an inertia tensor of the axial asymmetry, which gives rise to mixings of K -projections of the total spin J .³⁵⁾ The resultant motion should be called as "wobbling mode".²¹⁾ The energy spectrum is displayed in Fig. 9(b), compared with the spectrum without K -mixing in Fig. 9(a). Now the states of low lying K -series are not the eigenstates by themselves, but are recomposed into new states. It is very interesting that we again obtain several states including the $K = 0$ component as a result of K -mixing, which should show up themselves in the scattering. Those states are closely located in energy and so in good agreement with several fine peaks observed in the experiment. It should be noted here that due to the lack of the enough information about the deformations of the total system, we assumed the same parameter for the coupling strength Δ for the molecular ground-band states and for the butterfly states, although the extent of asymmetry is generally different in each band. As for the magnitudes of the moments of inertia (I_x, I_y, I_z), we estimated them as follows. We assumed a constant value for the relative distance, i.e., for μR^2 , and adopted $R = R_e = 7.6\text{fm}$. For the contributions from the moments of inertia of the constituent ^{28}Si nuclei, we estimated them about the y - and z -axes from the excitation energy of their 2_1^+ state. As for the contribution about x -axis, we assumed a factor $4/3$ larger than those about the other axes, due to the distribution of the nuclear density of ^{28}Si . For calculations

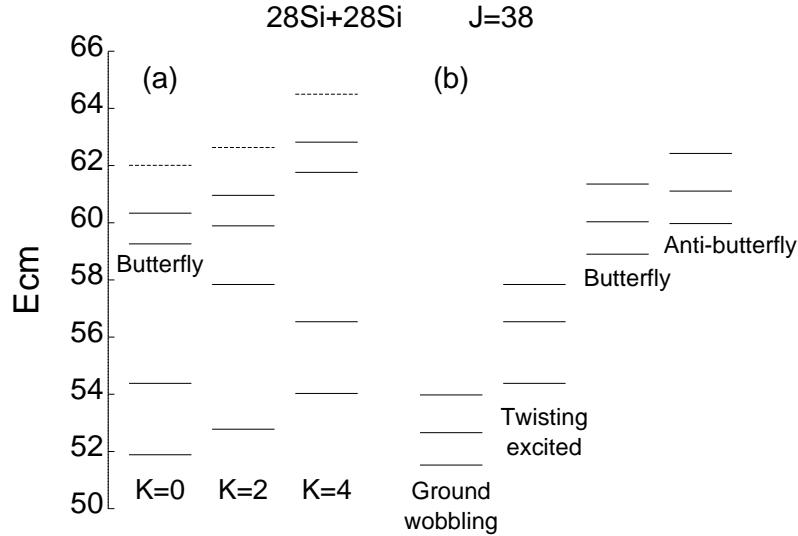


Fig. 9. Energy spectra of the $^{28}\text{Si} + ^{28}\text{Si}$ system for $J = 38$. (a) Molecular normal modes without K -mixing. (b) After K -mixing, with indications of the modes under the levels.

about the moments of inertia of dinuclear systems, details are given in Appendix D.

As an analytical prescription, in the high spin limit ($K/J \sim 0$), the diagonalization in the K -space is found to be equivalent to solving a differential equation of the harmonic oscillator with parameters given by the moments of inertia. Thereby, the solution is a gaussian, or a gaussian multiplied by an Hermite polynomial,

$$f_n(K) = H_n \left(\frac{K}{b} \right) \exp \left[-\frac{1}{2} \left(\frac{K}{b} \right)^2 \right], \quad (4.7)$$

where the width b is given by

$$b = (2J^2 I_K / \Delta)^{1/4}. \quad (4.8)$$

The eigenenergy E_n is approximately given by

$$E_n = \frac{J(J+1)\hbar^2}{2I_{av}} - \frac{J^2\hbar^2}{2\Delta} + \sqrt{\frac{2}{\Delta \cdot I_K}} J\hbar^2 \left(n + \frac{1}{2} \right), \quad (4.9)$$

where the second term on the r.h.s. is due to the coupling energy between the states with $\Delta K = 2$, which is approximated by $K/J = 0$. The third term is due to the energy of the harmonic oscillator, with the energy quantum,

$$\hbar\omega = \sqrt{\frac{2}{\Delta \cdot I_K}} J\hbar^2. \quad (4.10)$$

Its excitation should be with $n = \text{even}$ due to the symmetry between the $|K\rangle$ and $|-K\rangle$ components. Note that by the approximation $J(J+1) \sim J^2$ for the second term of the r.h.s. of Eq. (4.9), the first and second terms can be amalgamated into $J(J+1)\hbar^2/2I_x$, which reminds that the moment of inertia of the rotation is I_x . Considering $I_x \sim I_y$, i.e., $I_K^{-1} \sim (I_z^{-1} - I_x^{-1})$, the energy quantum $\hbar\omega$ of Eq. (4.10) is equivalent to that of the wobbling formula given in Ref. 35).

In order to calculate angular correlations we use those analytic forms in Eq. (4.7), which is simple and intuitive way to understand the extent of K -mixing. Of course we can utilize numerical values obtained in the diagonalization procedure, but the values are almost the same as those given by the analytic form. For the lowest state $f_0(K)$ of Eq. (4.7), we have the wave function for the wobbling ground state as

$$\Psi_\lambda^{JM} \sim \sum_K \exp(-K^2/2b^2) D_{MK}^J(\theta_i) \chi_K(R, \alpha, \beta_1, \beta_2), \quad (4.11)$$

where in general, χ_K can be any molecular mode of triaxial deformations, such as the ground-state configuration (parallel equator-equator one), the butterfly mode and the anti-butterfly mode. The magnitude of b estimated by Eq. (4.8) is 1.85, for example, for the values of the moments of inertia used in the calculations for the energy spectrum in Fig. 9. This is the largest value expected, because we assumed a static configuration there, in which the zero-point motions of the twisting and butterfly modes are neglected. A note for the wobbling wave functions is given in the last part of Appendix C.

In Fig. 10, theoretical energy levels of the $^{28}\text{Si} + ^{28}\text{Si}$ system are compared with the experimental data in the resonance energy region.^{5),6)} From the left, (a) shows the molecular ground band followed with the wobbling excited states, (b) an excited band due to the twisting motion with $K = 0$, (c) the butterfly mode with wobbling and (d) the anti-butterfly mode with wobbling. Molecular configurations are well stable by the barrier up to $J = 40$, while with $J = 42$, an existence of the molecular resonance state is unlikely, as the zero-point energy of the radial motion is over the barrier top. Levels with $J = 38$ are connected by thin lines for eye-guide. On the right-hand side, the experimental data are displayed, where $J = 36 \sim 40$ indicate the spin assignments for the broad bumps.⁴⁾ We see the density of the resonance states in the data is well reproduced by the calculated eigenstates, which are due to the wobbling motion and the excitations of the internal modes, such as butterfly etc. Note that the existence of the excited states of the wobbling motion as resonance states depends upon the stability of the triaxial structure, and hence the numbers of those excited states taken up in Fig. 10 are not definitive.

From $J = 36$ up to $J = 40$, the anti-butterfly mode appears higher than the butterfly one as is discussed in §3.2. For those anti-butterfly states we do not display the excited states of the wobbling motion, because each eigenstate of the anti-butterfly mode appears as the excited state of the butterfly state in the α -motion, and thus the

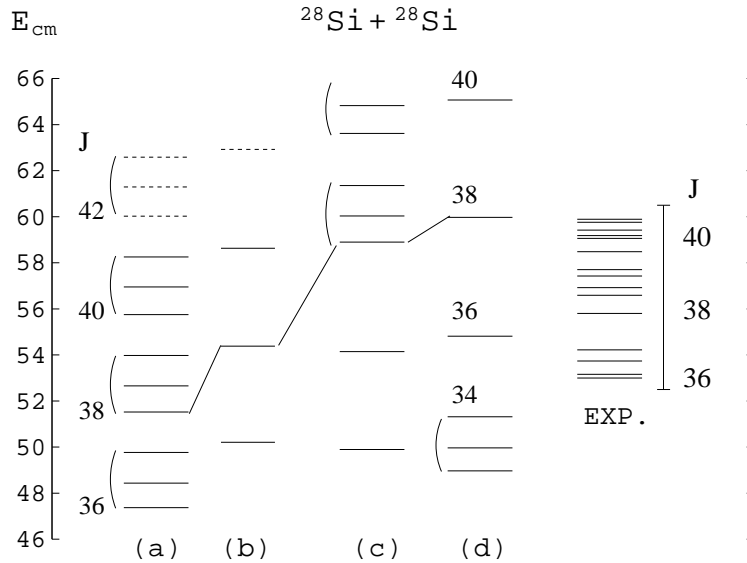


Fig. 10. Dinuclear spectrum of the $^{28}\text{Si} + ^{28}\text{Si}$ system in the resonance energy region is displayed. Levels with $J = 38$ are connected by thin lines for eye-guide. From the left, the resonance levels theoretically obtained, where (a) the members of the molecular ground band and of the wobbling excited bands, (b) an excited band due to the twisting motion with $K = 0$, (c) the butterfly mode with wobbling and (d) the anti-butterfly mode with wobbling. On the right-hand side, the experimental data are displayed, where $J = 36 - 40$ indicate the spin assignments for the broad bumps.⁴⁾ We selected resonance levels from the narrow peaks in the elastic and inelastic excitation functions, according to a statistical analysis on their correlation, with an indicative bar for the available energy region of the data.⁶⁾

configuration of the anti-butterfly mode is not enough triaxial. On the other hand, with $J = 34$ the anti-butterfly mode is lower in energy than the butterfly one, and thus we display the excited states of the wobbling motion for this mode. The reason of the lower excitation of the anti-butterfly mode is as follows. With relatively-low angular momentum, the constrain by the energy well around the equator-equator configuration becomes rather weak, and the stability of this configuration is not well guaranteed. We found that the equator-equator configuration is not at the local energy minimum below with $J = 32$. For example, with $J = 30$, the stable configuration for the molecular ground state is an antibutterfly-like one of $\beta \sim 60^\circ$, the equilibrium distance R_e of which is much smaller than that with $J = 34$. Such softening of the energy surface occurs with $J = 34$, which gives rise to lowering of the anti-butterfly mode.

4.2. *Comparison between the molecular-model hamiltonian and the asymmetric rotator's*

The wobbling motion associated with "K-mixing" is an important aspect of the rotation of the asymmetrically deformed nucleus in high spins. In order to investigate such an aspect, we have introduced the asymmetric rotator in addition to the molecular model, because the rotator model is simple to understand the essential feature of rotational motions. As the rotator model is based on more or less rigid intrinsic structure, it is interesting to know how the simple rotator model is related to the molecular model.

A triaxial system preferentially rotates around the axis with the largest moment of inertia. By the definition of the axes in the lower panel of Fig. 8, we have the moments of inertia of the total system as $I_X > I_Y \gg I_Z$ due to the configuration. Thus the total system, which is seen as two pancake-like objects touching side-by-side, rotates around the X -axis which is normal to the reaction plane. In this context, the magnitudes of the moments of inertia is crucially important; the large contributions to I_X from the third moments of inertia I_3 of the two constituent nuclei are expected. So here we study two examples of the molecular model, one of which is with $I_3 = 0$, and the other is with $I_3 \neq 0$.

We take up a resonant system consisting of "a spherical nucleus and a deformed nucleus". In order to see only the rotational motion, we assume that the two nuclei are bound and stay at a constant relative distance R , which reduces the degrees of freedom of the system. For the first example (case 1), an axially-symmetric deformation is assumed for the constituent nucleus, in which I_3 is taken to be zero. Thus the coordinates are taken as $(q_i) = (\theta_1, \theta_2, \theta_3, \beta)$, where θ_i denote the Euler angles for the rotation of the molecular axes. The internal degree of freedom is described with β . Those conditions are taken to be corresponding with the degrees of freedom in §2. On the other hand, in the second example (case 2), an axially-asymmetric deformation is assumed, i.e., I_3 is not zero, which gives rise to a degree of freedom γ . And then the coordinates are $(q_i) = (\theta_1, \theta_2, \theta_3, \beta, \gamma)$. Of course, the introduction of the γ -degree of freedom is an extension from the description in §2, which is expected from the nuclear density distribution illustrated in Fig. 8.

Typical configurations are illustrated in Fig. 11, where in (a), (b) and (c) the

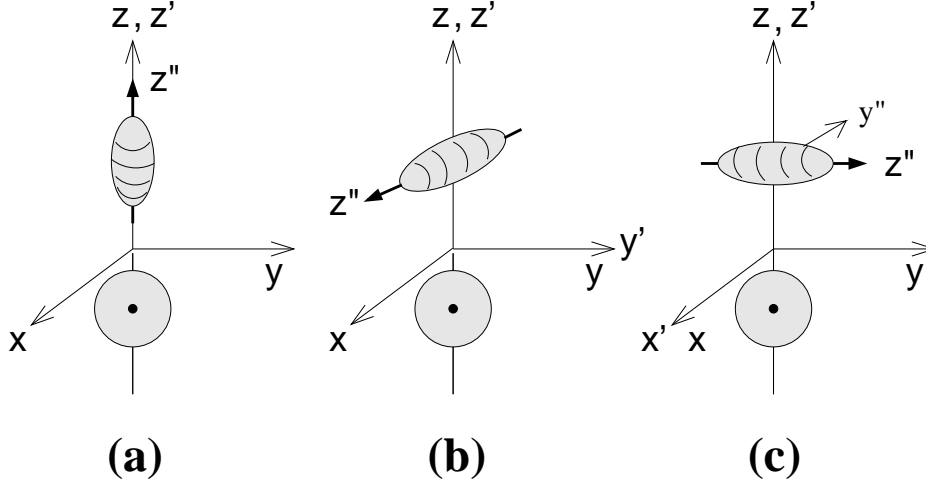


Fig. 11. Some examples for the geometrical configurations of the system consisting of a spherical nucleus and an axially-symmetric deformed nucleus. The molecular z' -axis is set to be parallel to the z -axis, as the whole rotation by $\Omega(\theta_1, \theta_2, \theta_3)$ will start with those configurations. In (a), the symmetry axis of the deformed nucleus (z'' -axis) is parallel to the z' -axis, due to the Euler rotations with $(\alpha, \beta) = (0, 0)$. In (b), the z'' -axis is parallel to the x' -axis, due to $(\alpha, \beta) = (0, \pi/2)$. In (c), the z'' -axis is parallel to the y' -axis, due to $(\alpha, \beta) = (\pi/2, \pi/2)$.

configurations are set with $(\alpha, \beta) = (0, 0)$, $(0, \pi/2)$ and $(\pi/2, \pi/2)$, respectively. The configuration (a) is axially symmetric for case 1, while those of (b) and (c) are axially asymmetric (the same shape). Note that the shape of the constituent deformed nucleus is prolate, but the figure is useful both for the prolate nucleus and for the oblate nucleus, of course. We describe the orientations of the principal axes of the constituent deformed nucleus with the Euler angles (α, β) , in which the degree of freedom associated with α is essentially the same as that associated with θ_3 of the total system, and thus α does not appear in (q_i) . Actually, the rotations of the whole system and the constituent nucleus are described by the relation,

$$\Omega_n(\tilde{\alpha}, \tilde{\beta}, \tilde{\gamma}) = \Omega'_n(\alpha, \beta, \gamma) \Omega_M(\theta_1, \theta_2, \theta_3), \quad (4.12)$$

where Ω_n and Ω'_n denote Euler rotations for the constituent deformed nucleus with respective angles, and Ω_M denotes rotations of the molecular axes. On the r.h.s. of Eq. (4.12), Ω'_n denote the successive rotation after Ω_M ; firstly the axes of the constituent deformed nucleus rotate up to the directions of the molecular axes by Ω_M , and secondly they rotate referring to the molecular axes by Ω'_n . Since the successive rotation is decomposed into $\Omega'_n(\gamma)\Omega'_n(\beta)\Omega'_n(\alpha)$, we have the rotations with angles θ_3 and α around the same axes obtained after $\Omega_M(\theta_1, \theta_2)$. Thus we can take the angle of the third rotation of the whole system simply to be $\theta_3 + \alpha$, which involve the freedom α . Here we regard the value of α as the initial condition for the starting configurations before rotation, which are displayed in Fig. 11.

We write the classical kinetic energy with the angular velocities, and then we replace these angular velocities with time derivatives of those coordinates (q_i) . The classical kinetic energy is expressed in the form $T = \frac{1}{2} \sum g_{ij} \dot{q}_i \dot{q}_j$ and we quantize it

by using the general formula for the curve-linear coordinate system. The quantum mechanical expression for the kinetic energy is given by

$$\hat{T} = -\frac{\hbar^2}{2} \sum_{ij} \frac{1}{\sqrt{g}} \frac{\partial}{\partial q_i} \sqrt{g} (g^{-1})_{ij} \frac{\partial}{\partial q_j}, \quad (4.13)$$

where g and g^{-1} denote the determinant and the inverse matrix of (g_{ij}) , respectively. The metric tensor (g_{ij}) is composed with the submatrices g_{rot} for the whole rotational degrees and g_{int} for the internal degrees of freedom as

$$(g_{ij}) = \begin{pmatrix} g_{rot} & g_C \\ {}^t g_C & g_{int} \end{pmatrix}, \quad (4.14)$$

where g_C denotes the nondiagonal part which corresponds to the Coriolis coupling, ${}^t g_C$ being the transpose of g_C . The way to obtain those components of g_{ij} is described in detail in Ref. 18). Here we briefly see their definitions:

$$g_{rot} = {}^t V(\theta_2, \theta_3) (\mathbf{I}_\mu + {}^t R(\alpha, \beta, \gamma) \mathbf{I}_n R(\alpha, \beta, \gamma)) V(\theta_2, \theta_3), \quad (4.15)$$

$$g_{int} = {}^t V(\beta, \gamma) \mathbf{I}_n V(\beta, \gamma), \quad (4.16)$$

$$g_C = {}^t V(\theta_2, \theta_3) {}^t R(\alpha, \beta, \gamma) \mathbf{I}_n V(\beta, \gamma), \quad (4.17)$$

where $V(\theta_2, \theta_3)$ and $V(\beta, \gamma)$ denote the transformation matrices between the derivatives of the Euler angles and the angular velocities of the molecular axes and of the constituent deformed nucleus, respectively, $R(\alpha, \beta, \gamma)$ being the rotation matrix. \mathbf{I}_μ denotes the inertia tensor for the two constituent nuclei as point-masses, i.e., the diagonal moments for x - and y -axes being μR^2 , while \mathbf{I}_n denotes the inertia tensor for the constituent deformed nucleus in its principal axes, respectively. The moments of inertia of the constituent deformed nucleus (the diagonal elements of \mathbf{I}_n) are taken as follows: for the axially symmetric nucleus (case 1), $I_1 = I_2 = I_0$ and $I_3 = 0$, and for the axially asymmetric nucleus (case 2), $I_1 = I_2 = I_0$ and the value of I_3 being not zero. For the latter case, in general, $I_1 \neq I_2$ may be used for the static asymmetric deformation, as was tried in the theory of the asymmetric rotator,²⁶⁾ but for simplicity we avoid this tedious calculations. Our consideration is focused on the appearance of the γ -degree of freedom associated with $I_3 \neq 0$, and for this purpose the assumption $I_1 = I_2$ brings no problem. Note that γ is spurious for the deformed nucleus with the axial symmetry, i.e., for case 1 with $I_3 = 0$. With the aid of mathematical software, we can easily obtain the elements g and $(g^{-1})_{ij}$, for example, $g = (\mu R^2)^2 I_0^2 \sin^2 \beta \sin^2 \theta_2$ for case 1, and $g = (\mu R^2)^2 I_0^2 I_3 \sin^2 \beta \sin^2 \theta_2$ for case 2, respectively.

As the classical kinetic energy consists of three parts, i.e., the rotation of the whole system, the internal motions and their couplings, the quantum mechanical operator for the kinetic energy \hat{T} is also given as a sum of three terms,

$$\hat{T} = \hat{T}_{rot} + \hat{T}_{int} + \hat{T}_C. \quad (4.18)$$

Naturally the term \hat{T}_{rot} is associated with the rotational variables $(\theta_1, \theta_2, \theta_3)$, \hat{T}_{int} with the internal variables (β, γ) and \hat{T}_C with both. According to the derivation, \hat{T}_{rot}

is expressed by the partial differential operators of θ_i . We combine those differential operators into angular momentum operators \hat{J}'_i . Thus we obtain the following kinetic energy terms,

$$\hat{T}_{\text{rot}} = \frac{\hbar^2}{2} \sum_{\substack{1 \leq i \leq 3 \\ 1 \leq j \leq 3}} \mu_{ij} \hat{J}'_i \hat{J}'_j, \quad (4.19)$$

where the matrix μ is the submatrix given later, and \hat{J}'_i are the angular momentum operators in terms of the Euler angles of the molecular frame, as usual, which is already given in Eq. (2.11). The coefficients μ_{ij} are determined due to the moments of inertia corresponding to the geometrical configuration, and are given in terms of the parameter α and the internal variable β as follows;

$$\begin{aligned} \mu_{11} &= \mu_{22} = \frac{1}{\mu R^2}, \\ \mu_{12} &= 0, \\ \mu_{13} &= \frac{1}{\mu R^2} \cos \alpha \cot \beta, \\ \mu_{23} &= \frac{1}{\mu R^2} \sin \alpha \cot \beta, \\ \mu_{33} &= \left(\frac{1}{I_0} + \frac{1}{\mu R^2} \right) \frac{1}{\sin^2 \beta} - \frac{1}{\mu R^2}. \end{aligned} \quad (4.20)$$

Note that the above expressions of μ_{ij} are the same between two examples, which are obtained under the assumption $I_1 = I_2 = I_0$.

The internal kinetic energy operator is associated with the variable β for case 1. We obtain

$$\hat{T}_{\text{int}}(\beta) = -\frac{\hbar^2}{2} \left(\frac{1}{I_0} + \frac{1}{\mu R^2} \right) \frac{\partial^2}{\partial \beta^2} - \frac{\hbar^2}{8} \left(\frac{1}{I_0} + \frac{1}{\mu R^2} \right) \left(\frac{1}{\sin^2 \beta} + 1 \right), \quad (4.21)$$

where the second term on the r.h.s. is the additional potential due to the new volume element $dV = d\beta$ instead of the original $dV = \mu R^2 I \sin \beta d\beta$. For the asymmetrically deformed constituent nucleus with $I_3 \neq 0$ (case 2), we have an additional term associated with the γ -degree of freedom, i.e.,

$$\hat{T}_{\text{int}}(\beta, \gamma) = \hat{T}_{\text{int}}(\beta) - \frac{\hbar^2}{2} \left\{ \frac{1}{\sin^2 \beta} \left(\frac{1}{I_0} \cos^2 \beta + \frac{1}{\mu R^2} \right) + \frac{1}{I_3} \right\} \frac{\partial^2}{\partial \gamma^2}, \quad (4.22)$$

where indications (β) and (β, γ) on \hat{T}_{int} are for distinction between cases 1 and 2.

The Coriolis coupling operator \hat{T}_{C} consists of coupling operators between the variables $(\theta_1, \theta_2, \theta_3)$ and β for case 1, i.e.,

$$\hat{T}_{\text{C}}(\theta_i; \beta) = -\frac{\hbar^2}{\mu R^2} \left\{ -\sin \alpha \left(-i \frac{\partial}{\partial \beta} \right) \hat{J}'_1 + \cos \alpha \left(-i \frac{\partial}{\partial \beta} \right) \hat{J}'_2 \right\}, \quad (4.23)$$

where the derivative operators of θ_i are rewritten with the angular momentum operators \hat{J}'_i . As for case 2, the couplings are between the variables $(\theta_1, \theta_2, \theta_3)$ and (β, γ) ,

for which we obtain

$$\begin{aligned} \hat{T}_C(\theta_i; \beta, \gamma) = \hat{T}_C(\theta_i; \beta) - \frac{\hbar^2}{\mu R^2 \sin \beta} & \left\{ \cos \alpha \left(-i \frac{\partial}{\partial \gamma} \right) \hat{J}'_1 + \sin \alpha \left(-i \frac{\partial}{\partial \gamma} \right) \hat{J}'_2 \right\} \\ & - \frac{\hbar^2}{\sin \beta} \cot \beta \left(\frac{1}{I_0} + \frac{1}{\mu R^2} \right) \left(-i \frac{\partial}{\partial \gamma} \right) \hat{J}'_3. \end{aligned} \quad (4.24)$$

Now we investigate those kinetic energy operators obtained. Firstly we proceed with case 1. Generally the hamiltonian of the system is composed of the kinetic energy and the interaction between the constituent nuclei $V(\beta)$, i.e.,

$$\hat{H} = \hat{T}_{\text{rot}} + \{\hat{T}_{\text{int}} + V(\beta)\} + \hat{T}_C. \quad (4.25)$$

Without the coupling \hat{T}_C , the internal motion is determined by the eigenvalue equation,

$$\hat{H}_{\text{int}} \chi(\beta) = \{\hat{T}_{\text{int}} + V(\beta)\} \chi(\beta) = E \chi(\beta). \quad (4.26)$$

For the case of a very strong confinement by the interaction $V(\beta)$, the motion associated with the β -degree is expected to approximately follow Eq. (4.26). And we write the rotational motion of the system, including \hat{T}_C , as

$$\hat{H}_{\text{rot}} = \hat{T}_{\text{rot}} + \hat{T}_C. \quad (4.27)$$

To analyze the rotational motion given by \hat{H}_{rot} , it is important to assume a dominant configuration such as the equator-equator one of the $^{28}\text{Si} + ^{28}\text{Si}$ system, which appears in low energy due to the interaction between the constituent nuclei. For we have all the possible rotational motions generally to appear in the energy spectrum of \hat{H}_{rot} , which make the problem extremely complicated. The dominant configuration assumed in this investigation is an axially asymmetric one with the strong confinement which is seen in Fig. 11(b) and/or Fig. 11(c). Thus we put $\beta \sim \pi/2$ for μ_{ij} of \hat{T}_{rot} in Eq. (4.20), i.e., $\cot \beta$ to be zero. As for α , its value is not essential, and we can choose any value for α . The Coriolis coupling $\hat{T}_C(\theta_i; \beta)$ of Eq. (4.23) reduces conveniently into one term, for the configuration with $\alpha = 0$ illustrated in Fig. 11(b), and we obtain

$$\hat{H}_{\text{rot}} = \frac{\hbar^2}{2} \left\{ \frac{J(J+1)}{\mu R^2} + \left(\frac{1}{I_0} - \frac{1}{\mu R^2} \right) \left(-\frac{\partial^2}{\partial \theta_3^2} \right) - \frac{2}{\mu R^2} \left(-i \frac{\partial}{\partial \beta} \right) \hat{J}'_2 \right\}, \quad (4.28)$$

where the first term of the r.h.s. is the angular momentum \hat{J}^2 replaced by $J(J+1)$, and the last term gives the Coriolis coupling. Note that for another configuration with $\alpha = \pi/2$ illustrated in Fig. 11(c), $-\hat{J}'_1$ appears instead of \hat{J}'_2 . In general, the Coriolis coupling induces K -mixing associated with the vibrational excitations, which is exemplified by the third term of the r.h.s. of Eq. (4.28); by using the creation and annihilation operators, a^* and a of the vibrational motion obtained by Eq. (4.26), the term is rewritten as $\sim (a^* - a)(\hat{J}_- - \hat{J}_+)$, where $\hat{J}'_{\pm} = \hat{J}'_1 \pm \hat{J}'_2$ are the lowering and raising operators of the K -quantum numbers. This description corresponds to that of the molecular hamiltonian given in §2.

On the other hand, there is a picture in which the internal degree β is frozen due to strong adhesion between the constituent nuclei, i.e., *the sticking limit*.²³⁾ In order to obtain relation to the rotator hamiltonian, we approach from such a picture, in which the sharing of the angular momenta is determined classically, i.e.,

$$\mathbf{J} = (\mu R^2 + I_0)\boldsymbol{\omega}, \quad \mathbf{L} = \mu R^2\boldsymbol{\omega}, \quad \mathbf{S} = I_0\boldsymbol{\omega}, \quad (4.29)$$

where $\boldsymbol{\omega}$ denotes the angular velocity of the whole system. Corresponding to the above relations, quantum mechanical ones are derived in Eq. (A.18) of Appendix A as follows,

$$\hat{\mathbf{S}}/I_0 = \hat{\mathbf{L}}/\mu R^2 = \hat{\mathbf{J}}/(\mu R^2 + I_0), \quad (4.30)$$

where $\hat{\mathbf{S}}$, $\hat{\mathbf{L}}$ and $\hat{\mathbf{J}}$ denote the spin of the constituent deformed nucleus, the orbital and the total angular momenta, which are defined as the rotations on the same plane. Although the relations in Eq. (4.30) are limited among the rotations around the same axis, they are approximately applicable to the present analysis, because we are considering the rotation of the whole system around the largest moment of inertia; for example, the axis of the rotation is y' for the configuration in Fig. 11(b). Therefore $\hat{\mathbf{S}}$ is associated with the β -degree, and $\hat{\mathbf{J}}$ corresponds to \hat{J}'_2 with respect to the configuration in Fig. 11(b). Following Eq. (4.30), we use a relation,

$$\left(-i\frac{\partial}{\partial\beta}\right)/I_0 = \hat{J}'_2/(\mu R^2 + I_0), \quad (4.31)$$

and rewrite the total kinetic energy $\hat{T} = \hat{T}_{\text{rot}} + \hat{T}_{\text{int}} + \hat{T}_{\text{C}}$. Then the result turns out to be the hamiltonian of the asymmetric rotator, i.e.,

$$\hat{T} = \frac{\hbar^2}{2} \left\{ \frac{(\hat{J}'_1)^2}{\mu R^2} + \frac{(\hat{J}'_2)^2}{\mu R^2 + I_0} + \frac{(\hat{J}'_3)^2}{I_0} \right\}. \quad (4.32)$$

Note that due to the configuration in Fig. 11(b), we put $\alpha = 0$ and $\beta = \pi/2$ for μ_{ij} of \hat{T}_{rot} in Eq. (4.20), and $\hat{T}_{\text{C}}(\theta_i; \beta)$ of Eq. (4.23), respectively. Note also that we drop the additional potential in $\hat{T}_{\text{int}}(\beta)$ (the second term of the r.h.s. of Eq. (4.21)), because the new volume element is not applied for the spin degree of freedom β . Thus we successfully obtained the asymmetric rotator hamiltonian. However, \hat{T} in Eq. (4.32) is too simple, because the β -degree is frozen and disappears. So this way does not exactly correspond to what is shown in §4.1. There we have the hamiltonian for the activated β -degrees in addition to the rotator one. Although the above \hat{T} in Eq. (4.32) is well correspondent to the kinetic energy operator given in §2.2 and gives a rotator hamiltonian, eventually, the results of the diagonalization of \hat{T}_{C} in §2.2 may not give rise to the energy spectrum given in Fig. 9.

Next we examine the case 2, in which two internal degrees of freedom (β, γ) are treated. In Fig. 12, the configuration with the oblate deformed constituent nucleus is illustrated corresponding to Fig. 11(b), where a larger value of I_3 than that of I_0 is assumed. So the axis with the largest moment of inertia is x' in this case. According to the configuration, we again put $\alpha = 0$ and $\beta = \pi/2$ into \hat{T}_{rot} , $\hat{T}_{\text{int}}(\beta, \gamma)$ and $\hat{T}_{\text{C}}(\theta_i; \beta, \gamma)$, respectively, which gives

$$\hat{T}_{\text{int}}(\beta, \gamma) = -\frac{\hbar^2}{2} \left\{ \left(\frac{1}{I_0} + \frac{1}{\mu R^2} \right) \left(\frac{\partial^2}{\partial\beta^2} + \frac{1}{2} \right) + \left(\frac{1}{I_3} + \frac{1}{\mu R^2} \right) \frac{\partial^2}{\partial\gamma^2} \right\}, \quad (4.33)$$

and

$$\hat{T}_C(\theta_i; \beta, \gamma) = -\frac{\hbar^2}{\mu R^2} \left\{ \left(-i \frac{\partial}{\partial \beta} \right) \hat{J}'_2 + \left(-i \frac{\partial}{\partial \gamma} \right) \hat{J}'_1 \right\}. \quad (4.34)$$

We again proceed in the picture of the sticking limit. Relations similar to Eq. (4.29) are assumed as follows:

$$\mathbf{J} = (\mu R^2 + I_3) \boldsymbol{\omega}, \quad \mathbf{L} = \mu R^2 \boldsymbol{\omega}, \quad \mathbf{S} = I_3 \boldsymbol{\omega}, \quad (4.35)$$

where $\boldsymbol{\omega}$ denotes the angular velocity of the whole system again, the rotation being around the x' -axis. Due to the same relation as Eq. (4.30) except I_0 being replaced with I_3 , we use a relation,

$$\left(-i \frac{\partial}{\partial \gamma} \right) / I_3 = \hat{J}'_1 / (\mu R^2 + I_3). \quad (4.36)$$

By Eq. (4.36), only the γ -degree is frozen out, and as a result we obtain the total kinetic energy operator,

$$\begin{aligned} \hat{T} = & \frac{\hbar^2}{2} \left\{ \frac{(\hat{J}'_1)^2}{\mu R^2 + I_3} + \frac{(\hat{J}'_2)^2}{\mu R^2} + \frac{(\hat{J}'_3)^2}{I_0} \right\} \\ & - \frac{\hbar^2}{2} \left(\frac{1}{I_0} + \frac{1}{\mu R^2} \right) \left(\frac{\partial^2}{\partial \beta^2} + \frac{1}{2} \right) - \frac{\hbar^2}{\mu R^2} \left(-i \frac{\partial}{\partial \beta} \right) \hat{J}'_2. \end{aligned} \quad (4.37)$$

Thus we finally obtain the asymmetric rotator hamiltonian accompanied by the vibrational mode β . It is noted that the equilibrium of the β -vibration is assumed to be $\beta = \pi/2$ in the derivation. In this model, the pole orientation of the constituent deformed nucleus is fluctuating around the direction of x' -axis seen in Fig. 12, while the whole system with the moment of inertia $\mu R^2 + I_3$ rotates approximately around the x' -axis with rather confined configuration. This is just the same picture adopted in §4.1, where the two constituent nuclei keep in touch and are sticking in the rotational motions along the same axis as the whole rotating system. As for the moments of inertia of the system, strong confinements due to the nucleus-nucleus interaction are supposed to give rise to induced deformations and/or a neck formation of the constituent nuclei, which bring nonzero moments I_3 of the constituent nuclei in addition to the original moments I_0 of the deformed nuclei with the axial symmetry. Thus, we expect that the above analysis is physically meaningful.

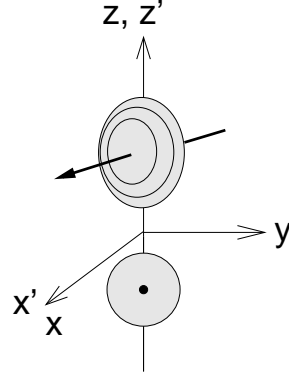


Fig. 12. An example for the geometrical configurations of the system consisting of a spherical nucleus and a nucleus with oblate deformation, for intuitive understanding. The molecular z' -axis is set to be parallel to the z -axis, and the symmetry axis of the deformed nucleus (z'' -axis) is parallel to the x' -axis, due to $(\alpha, \beta) = (0, \pi/2)$.

§5. Summary

The interaction between two nuclei is described with the internal collective variables, i.e., the orientations of the poles of the constituent nuclei in the rotating molecular frame. In the dinuclear system with oblate-deformed constituent nuclei, an equator-equator touching configuration with the parallel principal axes is found to be the equilibrium at high spins. In the $^{28}\text{Si} + ^{28}\text{Si}$ system, the relative distance between the two ^{28}Si nuclei is 7 – 8fm, indicating a nuclear compound system with hyperdeformation. The barrier position is 9 – 10fm, greatly outside from that of usual optical potentials. Molecular configurations are well stable by the barrier up to $J = 40$, while with $J = 42$, an existence of the molecular resonance state with narrow widths is unlikely, as the zero-point energy of the radial motion is over the barrier top. This theoretical maximum spin is in accord with the bumps observed in grazing angular momenta.

Couplings among various molecular configurations are taken into account by the method of normal mode around the equilibrium configuration, which gives rise to the molecular modes of excitation, such as the radial vibration, the butterfly motion, the anti-butterfly motion and so on. The twisting mode ($\nu = 4$) is found to be the lowest excitation. Vibrational energy quanta for the butterfly and the anti-butterfly modes are about 4MeV, but the excitation energies of those modes have to be twice, 8MeV, since states of $K = \text{even}$ with one vibrational quantum are not allowed due to the boson symmetry. Thus, the energies are close to those for the radial excitation. Although the excited state of the radial mode is not bound in the present calculations, the possibility of the radial-mode resonance is not completely excluded, because it is likely that the interaction between two ^{28}Si would be more attractive than the present folding potential with the frozen density.

A triaxial system preferentially rotates around the axis with the largest moment of inertia. By the definition of the axes in the lower panel of Fig. 8, we have the moments of inertia of the total system as $I_X > I_Y \gg I_Z$. Thus the total system, which is seen as two pancake-like objects touching side-by-side, rotates around the X-axis which is normal to the reaction plane. As the axial symmetry is slightly broken, wobbling motion appears in that way.

We extend our molecular model so as to include couplings between states with different K -quantum numbers. Usually, the Coriolis coupling terms are diagonalized, but we do not treat them explicitly. In practice, we use the asymmetric rotator as an intuitive model. By the diagonalization of the rotator hamiltonian in the K -space, we obtain new low-lying states due to a triaxial shape of the equilibrium configuration. In the high spin limit ($K/J \sim 0$), the diagonalization is found to be equivalent to solving a differential equation of the harmonic oscillator with spring constants given by the moments of inertia. Thereby, the analytic solution is obtained to be a gaussian, or a gaussian multiplied by an Hermite polynomial, which is a useful tool for the analyses of the molecular states with the triaxial configuration.

Since the Coriolis terms in the molecular hamiltonian appear to be quite different from the asymmetric rotator, it is necessary and meaningful to study the relations between the molecular hamiltonian and the asymmetric rotator's. The analysis turns

out that the hamiltonian of the molecular model with the γ -degree of freedom reduces to that of an asymmetric rotator in the sticking limit.²³⁾ Thus the intuitive use of the asymmetric rotator is warranted, and it provides a very simple understanding with easy calculations of the effects of K -mixing on the energy spectrum.

Finally it should be mentioned that an extension of the molecular model is possible so as to include the γ_i -degrees of freedom. For example, possible γ -vibrations of the constituent nuclei could be taken into account. But we do not include those surface vibrations and the corresponding γ_i -degrees of freedom, considering that the dominances of the members of the ground-state band in the decays are reported for the $^{28}\text{Si} + ^{28}\text{Si}$ system⁹⁾ and for the $^{24}\text{Mg} + ^{24}\text{Mg}$ system,³⁶⁾ respectively. A molecular model with two asymmetric rotators of the constituent nuclei is not pursued for the moment, which does not appear rewarding for elaboration. Furthermore, the constituent nuclei are expected to be strongly confined to form the whole deformed system, in which the γ_i -degrees of freedom are approximately frozen. Hence, we adopt the asymmetric rotator for the whole system as a sticking limit of the γ_i -degrees of freedom.

We have intuitively expected that the moment of inertia I_X is the largest for the configuration in Fig. 8. Namely, we implicitly assume $I_1 \neq I_2$ and $I_3 \neq 0$ for the moments of inertia of the constituent nuclei in their principal axes, due to additional deformations likely induced by the interactions at the contact configurations of the two nuclei, while in §2, without the induced deformations, we have assumed the axial symmetry of ^{28}Si and the intrinsic moment $I_3 = 0$. (The latter gives $I_Y > I_X \gg I_Z$.) The dynamical process of the transition between those two states of the constituent nuclei with $I_3 = 0$ and $I_3 \neq 0$ is an interesting problem, which should be clarified in future. The nuclear structure with large induced deformations may be close to that obtained by the Nilsson-Strutinsky calculations for ^{56}Ni .¹²⁾ However the experiments exhibit the nature of the dinuclear complex in resonances, i.e., the dominance of binary decays,⁹⁾ which suggests the contact of the two ^{28}Si nuclei is not violent enough for rearrangements of the nuclear structure of the constituent nuclei in the molecular model.

The molecular states obtained in the present paper are expected to be the origin of a large number of resonances observed, and hence theoretical analyses have been made for the angular distributions and the angular correlations. The results have been compared with the recent experiment performed in Strasbourg^{9), 22)} to give good agreements with the data, which will be given in the succeeding paper.²⁴⁾

Acknowledgements

The authors thank Drs. C. Beck, R. Freeman and F. Haas for stimulating discussions in their collaborations. The authors are grateful for the discussion and for the hospitality of Dr. B. Giraud in the visits at Saclay.

This work was supported in part by the Grant-in-Aid for Scientific Research from the Japanese Ministry of Education, Culture, Sports, Science and Technology (12640250).

Appendix A

— Relation between the Coordinate Systems and the Angular Momentum Operators in the Molecular Model —

In the present appendix, the description of the angular momenta for the total kinetic energy operator in the molecular model is ascertained with respect to the coordinate system. For this purpose, we take up a two-body problem in which one body is deformed and has own rotational degrees of freedom. In the laboratory frame the description of the kinetic energy of the system is rather simple as we consider the energies from the rotational motion of the two-body relative vector (orbital motion) and the spin degrees separately. However in the body-fixed frame, i.e., in the molecular frame, the description is not so easy, because the total system is not simple as a rigid rotator. Firstly, the coordinates for the molecular frame and those of the

internal degrees of freedom associated with the frame should be chosen appropriately. Secondly, although we can obtain the kinetic energy operator \hat{T} by using the formula for the curve-linear coordinates which is given later in Eq. (A·3), we have three parts of \hat{T} , i.e., the rotational energy, the energy associated with the internal degrees of freedom and the couplings between them, the roles of which have to be clarified. As is shown below, the property of the operator, for example, to be the total angular momentum or to be the orbital angular momentum, is determined not only by the coordinates for the rotational motions themselves but also by the moments of inertia associated with. This is natural as the angular momentum in the classical description. Two examples are given; one is for the present molecular frame, and the other is for a new molecular frame, in which the couplings between the whole rotation and the internal motions disappear.

Consider a resonant system consisting of "a spherical nucleus and an axially-symmetric deformed nucleus". In order to see the rotational motion, we assume that the two nuclei are bound and stay at a constant relative distance R , which reduces the degrees of freedom of the system. To limit the degrees of freedom to be "two dimensional", we again assume that the symmetry axis of the deformed nucleus is in the reaction plane. As is illustrated in Fig. 13, referring to the space-fixed axes, the orientation of the relative vector of the two constituent nuclei is described by the angle θ_0 , and the angle of the orientation of the symmetry axis is denoted as α_0 . The classical kinetic energy is given with two angular velocities $\omega = \dot{\theta}_0$ and $\omega_n = \dot{\alpha}_0$, as $T = 1/2 \cdot (\mu R^2 \omega^2 + I_n \omega_n^2)$, where μ and I_n denote the reduced mass of the two nuclei

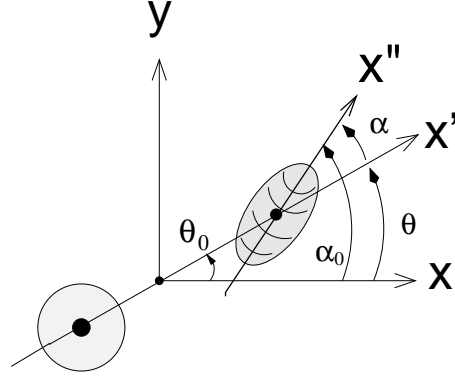


Fig. 13. The Coordinates of the system which consists of a spherical nucleus and a deformed nucleus with axial symmetry. Both the relative vector and the symmetry axis of the deformed nucleus are assumed to be parallel to the xy -plane.

and the moment of inertia of the deformed nucleus, respectively. The corresponding kinetic energy operator is given by

$$\hat{T} = \frac{\hbar^2}{2\mu R^2} \mathbf{L}^2 + \frac{\hbar^2}{2I_n} \mathbf{S}^2, \quad (\text{A}\cdot 1)$$

where \mathbf{L} and \mathbf{S} denote the orbital angular momentum and the spin of the deformed nucleus, as usual. Note that by definition, the angular momenta are those for the one dimensional rotations, i.e., they are given by $\mathbf{L} = -i\partial/\partial\theta_0$ and $\mathbf{S} = -i\partial/\partial\alpha_0$, respectively.

In the description by the molecular model, we take the molecular x' -axis which is parallel to the relative vector of the two nuclei, as illustrated in Fig. 13, and the coordinate is denoted as θ (the angle θ is the same as θ_0 , i.e., $\theta = \theta_0$). And the angle of the orientation of the symmetry axis is described referring to the molecular x' -axis as $\alpha = \alpha_0 - \theta_0$. Then due to $\omega'_n = \omega_n - \omega$ with $\omega'_n = \dot{\alpha}$ and $\omega = \dot{\theta}$, the classical kinetic energy is written as

$$T = \frac{1}{2}(I_{\text{total}} \omega^2 + 2I_n \omega \omega'_n + I_n \omega_n'^2), \quad (\text{A}\cdot 2)$$

where I_{total} denotes the moment of inertia of the whole system given by $I_{\text{total}} = \mu R^2 + I_n$. Replacing these angular velocities with time derivatives of the coordinates $(q_i) = (\theta, \alpha)$, we write a classical kinetic energy in the form $\frac{1}{2} \sum g_{ij} \dot{q}_i \dot{q}_j$. And then we quantize it by using the general formula for the curve-linear coordinate system,

$$\hat{T} = -\frac{\hbar^2}{2} \sum_{ij} \frac{1}{\sqrt{g}} \frac{\partial}{\partial q_i} \sqrt{g} (g^{-1})_{ij} \frac{\partial}{\partial q_j}, \quad (\text{A}\cdot 3)$$

where g and g^{-1} denote the determinant and the inverse matrix of (g_{ij}) , respectively. In this case, the metric tensor is given by

$$(g_{ij}) = \begin{pmatrix} \mu R^2 + I_n & I_n \\ I_n & I_n \end{pmatrix}, \quad (\text{A}\cdot 4)$$

and hence the inverse matrix is obtained as

$$(g_{ij})^{-1} = \begin{pmatrix} 1/\mu R^2 & -1/\mu R^2 \\ -1/\mu R^2 & 1/\mu R^2 + 1/I_n \end{pmatrix}. \quad (\text{A}\cdot 5)$$

As the classical kinetic energy consists of the three parts, i.e., the rotation of the whole system, the internal motions and their couplings, the quantum mechanical operator for the kinetic energy \hat{T} is also given as a sum of three terms, which appears to be

$$\hat{T} = -\frac{\hbar^2}{2} \left\{ \frac{1}{\mu R^2} \frac{\partial^2}{\partial \theta^2} - \frac{2}{\mu R^2} \frac{\partial^2}{\partial \theta \partial \alpha} + \left(\frac{1}{\mu R^2} + \frac{1}{I_n} \right) \frac{\partial^2}{\partial \alpha^2} \right\}. \quad (\text{A}\cdot 6)$$

We define the total angular momentum \mathbf{J}_θ and the operator for the internal (rotational or vibrational) motion of the deformed nucleus \mathbf{S}_α , by $\mathbf{J}_\theta = -i\partial/\partial\theta$ and

$\mathbf{S}_\alpha = -i\partial/\partial\alpha$, respectively, and rewrite Eq. (A·6) with those operators as follows,

$$\hat{T} = \frac{\hbar^2}{2} \{ \mathbf{J}_\theta^2 / \mu R^2 - 2\mathbf{J}_\theta \mathbf{S}_\alpha / \mu R^2 + (1/\mu R^2 + 1/I_n) \mathbf{S}_\alpha^2 \} \quad (\text{A} \cdot 7)$$

$$= \frac{\hbar^2}{2\mu R^2} (\mathbf{J}_\theta - \mathbf{S}_\alpha)^2 + \frac{\hbar^2}{2I_n} \mathbf{S}_\alpha^2, \quad (\text{A} \cdot 8)$$

which corresponds to Eq. (A·1) and exhibits the role of the Coriolis terms in the molecular model. Note that the coordinate θ for the molecular x' -axis is the same angle as θ_0 , but the role of θ is different from θ_0 . The molecular axis $x'(\theta)$ represents the motion of the whole system with the moment of inertia I_{total} , while θ_0 is the angle of the relative vector between the two constituent nuclei, which represents the orbital motion. The process by using the formula Eq. (A·3) of the general quantization for the curve-linear coordinates gives a simple example for the kinetic energy operator described in §2, which clarifies the property of the molecular coordinate θ .

We can introduce the angular momentum operators \mathbf{J}_θ and \mathbf{S}_α , of course, by the direct transformation for the differential operators. We obtain, due to the relations between the arguments ($\theta_0 = \theta, \alpha_0 = \theta + \alpha$),

$$\frac{\partial}{\partial\theta} = \frac{\partial\theta_0}{\partial\theta} \frac{\partial}{\partial\theta_0} + \frac{\partial\alpha_0}{\partial\theta} \frac{\partial}{\partial\alpha_0} = \frac{\partial}{\partial\theta_0} + \frac{\partial}{\partial\alpha_0}, \quad (\text{A} \cdot 9)$$

$$\frac{\partial}{\partial\alpha} = \frac{\partial\theta_0}{\partial\alpha} \frac{\partial}{\partial\theta_0} + \frac{\partial\alpha_0}{\partial\alpha} \frac{\partial}{\partial\alpha_0} = \frac{\partial}{\partial\alpha_0}, \quad (\text{A} \cdot 10)$$

and accordingly we can confirm the relations, $\mathbf{J}_\theta = \mathbf{L} + \mathbf{S}$ and $\mathbf{S}_\alpha = \mathbf{S}$. As for the wave functions, let us start those with the eigenvalues M and m for \mathbf{L} and \mathbf{S} , respectively. The total wave function Ψ is defined by $\Psi(\theta_0, \alpha_0) = N e^{iM\theta_0} e^{im\alpha_0}$, the arguments of which could be replaced by the coordinate transformation as ($\theta_0 = \theta, \alpha_0 = \theta + \alpha$), and accordingly we obtain $\Psi(\theta, \alpha) = N e^{iM\theta} e^{im(\theta+\alpha)} = N e^{i(M+m)\theta} e^{im\alpha}$. Note that the function $e^{im\alpha}$ is the same one obtained from the operation of the unitary transformation of the whole rotation $\hat{R}_n(\theta) = e^{-i\theta(\mathbf{n} \cdot \mathbf{S})}$ on the spin function in the laboratory system, i.e., $\hat{R}_n(\theta) e^{im\alpha_0} = e^{im\alpha}$, where \mathbf{n} denotes the unit vector normal to the plane. (For the general rotations in three dimensional space, the transformations are described by D -functions.) The resultant part $e^{i(M+m)\theta}$ properly corresponds to the wave function for the degree of freedom of "the whole rotation of the system", and thus we again confirm that the eigenvalue J of \mathbf{J}_θ satisfies the usual rule $J = M + m$.

In the molecular model, firstly we consider the whole rotating system with a stable (equilibrium) configuration expected, and secondly we investigate the internal degrees of freedom associated with it. With the strong nucleus-nucleus interaction, the motions of the constituent nuclei may be perfectly confined, and hence we sometimes consider the internal degrees of freedom to be frozen, i.e., *the sticking limit*.²³⁾ Thus it is worth while looking the kinetic energy of the molecular model in the sticking limit. In the classical kinetic energy Eq. (A·2), we put $\omega'_n = 0$ ($\omega = \omega_n$) and accordingly we obtain the energy of the rotator $T = I_{\text{total}}\omega^2/2$. However, in the quantum mechanical expression in Eq. (A·6) and/or (A·8), it is clear above that

the molecular model does not directly correspond to the sticking model, because the rotational energy is not given by $\mathbf{J}^2 \hbar^2 / 2I_{\text{total}}$. To make a model corresponding to the sticking model in quantum mechanics, we define a new coordinate Θ , "the angle for the center of the moments of inertia" in stead of the Euler angle θ for the molecular z' -axis, as $\Theta = (\mu R^2 \cdot \theta_0 + I_n \cdot \alpha_0) / (\mu R^2 + I_n)$. The other coordinate is again "the internal angle" $\alpha' = \alpha_0 - \theta_0$, which is the same as in the molecular model, and the corresponding moment of inertia is given by $I_{\text{internal}} = \mu R^2 \cdot I_n / (\mu R^2 + I_n)$. The set of the coordinates (Θ, α') gives the classical kinetic energy expression without the Coriolis coupling term, as

$$T = \frac{1}{2}(I_{\text{total}}\Omega^2 + I_{\text{internal}}\omega_n'^2), \quad (\text{A}\cdot 11)$$

where Ω denotes the angular velocity $\dot{\Theta}$. Thus we obtain the kinetic energy operator

$$\hat{T} = \frac{\hbar^2}{2I_{\text{total}}}\mathbf{J}_{\Theta}^2 + \frac{\hbar^2}{2I_{\text{internal}}}\mathbf{S}_{\alpha'}^2, \quad (\text{A}\cdot 12)$$

where by putting $\mathbf{S}_{\alpha'} = 0$ we reach the kinetic energy of the rigid-rotator type. Note that the choice of those coordinates follows the usage of the center of mass coordinate and the relative vector for two-body problem. Unfortunately this set of the coordinates would be limited on the rotations in a plain, because it is not easy to define "the center of the moments of inertia" for the multi-dimensional internal rotations. Now, by the direct transformation for the differential operators, we again calculate operators \mathbf{J}_{Θ} and $\mathbf{S}_{\alpha'}$ due to the relations

$$\theta_0 = \Theta - I_n / (\mu R^2 + I_n) \cdot \alpha', \quad (\text{A}\cdot 13)$$

$$\alpha_0 = \Theta + \mu R^2 / (\mu R^2 + I_n) \cdot \alpha', \quad (\text{A}\cdot 14)$$

which appear as

$$\frac{\partial}{\partial \Theta} = \frac{\partial}{\partial \theta_0} + \frac{\partial}{\partial \alpha_0}, \quad (\text{A}\cdot 15)$$

$$\frac{\partial}{\partial \alpha'} = -\frac{I_n}{\mu R^2 + I_n} \frac{\partial}{\partial \theta_0} + \frac{\mu R^2}{\mu R^2 + I_n} \frac{\partial}{\partial \alpha_0}. \quad (\text{A}\cdot 16)$$

Thus again we have a usual description for the total angular momentum associated with Θ as a sum of the orbital angular momentum and the spin, i.e., $\mathbf{J}_{\Theta} = \mathbf{L} + \mathbf{S}$. As for the spin for the internal rotation $\mathbf{S}_{\alpha'}$, the definition turns out to be

$$\mathbf{S}_{\alpha'} = -i\partial/\partial\alpha' = (\mu R^2 \cdot \mathbf{S} - I_n \cdot \mathbf{L}) / (\mu R^2 + I_n). \quad (\text{A}\cdot 17)$$

For the sticking limit, we put $\mathbf{S}_{\alpha'} = 0$, and then we obtain

$$\mathbf{S}/I_n = \mathbf{L}/\mu R^2 = \mathbf{J}/(\mu R^2 + I_n), \quad (\text{A}\cdot 18)$$

which is known as the rule of angular momentum sharing in the sticking model.²³⁾ Thus the coordinate system taken up here properly gives the whole rotation and the internal motion without the coupling as a quantum mechanical description of the sticking model.

Appendix B

— Symmetries of the System and Construction of the Wave Functions —

Here we deal with symmetry properties of the system and their associated restrictions on the wave function, from which selection rules for quantum numbers are deduced. Following those results, practical expressions for wave functions are given in the next Appendix C.

Firstly we note the coordinate transformation rules for boson and parity operations in the molecular frame. Here we do not describe how to obtain the rules. One could refer the derivations given in the Appendix D of Ref. 18).

Boson symmetry

We have the exchange operator \mathcal{P}_{12} , which acts on both the molecular coordinates and the internal variables, and transforms them as follows;

$$\mathcal{P}_{12} : (\theta_1, \theta_2, \theta_3, \alpha, R, \beta_1, \beta_2) \rightarrow (\pi + \theta_1, \pi - \theta_2, -\theta_3, \alpha, R, \pi - \beta_2, \pi - \beta_1). \quad (\text{B}\cdot 1)$$

Inversion symmetry (parity)

The inversion operator \mathcal{P} acts as follows;

$$\mathcal{P} : (\theta_1, \theta_2, \theta_3, \alpha, R, \beta_1, \beta_2) \rightarrow (\pi + \theta_1, \pi - \theta_2, \pi - \theta_3, -\alpha, R, \beta_1, \beta_2). \quad (\text{B}\cdot 2)$$

Wave functions of the system with good symmetries

Since the axial symmetry of constituent nuclei is assumed, the variables γ_i are not necessary. Each nucleus has positive parity, and thus its density profile is invariant under space inversion. Accordingly, the basis wave function $D_{MK}^J(\theta_i)\chi_K(R, \alpha, \beta_1, \beta_2)$ should be invariant under the inversion operation upon a constituent nucleus,

$$\mathcal{I}_i : (\alpha_i, \beta_i) \rightarrow (\alpha_i + \pi, \pi - \beta_i). \quad (\text{B}\cdot 3)$$

Before we examine the symmetry for \mathcal{I}_i , it should be noted that the transformations \mathcal{I}_i affect the rotational variable θ_3 as well as the internal variables α, β_1 and β_2 , because orientation of the molecular x' -axis changes according to a change of the orientation of a constituent nucleus. For example, we take up $\mathcal{I}_1^2 : (\alpha_1, \beta_1) \rightarrow (\alpha_1 + 2\pi, \beta_1)$, which should be equal to unity, because it gives just 2π rotation of one constituent nucleus around the molecular z' -axis. By operating \mathcal{I}_1^2 on θ_3 and α of $D_{MK}^J(\theta_i)\chi_K(R, \alpha, \beta_1, \beta_2)$, according to $\theta_3 = (\alpha_1 + \alpha_2)/2$ and $\alpha = (\alpha_1 - \alpha_2)/2$, we obtain a cyclic condition including the factor from the transformation on θ_3 ,

$$D_{MK}^J(\theta_i)\chi_K(R, \alpha, \beta_1, \beta_2) = (-1)^K D_{MK}^J(\theta_i)\chi_K(R, \alpha + \pi, \beta_1, \beta_2). \quad (\text{B}\cdot 4)$$

Now in order to examine symmetries about the inversion operations \mathcal{I}_i , we set trial wave functions concretely. By introducing harmonic approximation with the variables $\beta_+ = (\Delta\beta_1 + \Delta\beta_2)/\sqrt{2}$ and $\beta_- = (\Delta\beta_1 - \Delta\beta_2)/\sqrt{2}$ with $\Delta\beta_i \equiv \beta_i - \pi/2$, the internal motions are described with

$$\chi_K(R, \alpha, \beta_1, \beta_2) = f_n(R)\phi_K(\alpha)\varphi_{n+}^+(\beta_+, \alpha)\varphi_{n-}^-(\beta_-, \alpha), \quad (\text{B}\cdot 5)$$

where n , n_+ and n_- denote oscillator quantum numbers, respectively. For $\chi_K(R, \alpha, \beta_1, \beta_2)$ of Eq. (B·5), Eq. (B·4) means as

$$\phi_K(\alpha) = (-1)^K \phi_K(\alpha + \pi). \quad (\text{B} \cdot 6)$$

Note that α -dependences in $\varphi_{n_+}^+$ and $\varphi_{n_-}^-$ originate from those in the oscillator hamiltonians $H_{\pm}(\beta_{\pm}, \alpha)$ for the β_+ and β_- degrees of freedom, which are almost separable from the α -degree but not completely, as is seen in Eqs. (3·5) – (3·8) in §3. Naturally, the periodical property of the α -degree of freedom is of period π . Furthermore due to the geometrical identification of the configurations specified with $\alpha = \pi/2$ and $\alpha = 0$, we have a relation between butterfly function $\varphi_{n_+}^+(\beta_+, \alpha)$ and anti-butterfly one $\varphi_{n_-}^-(\beta_-, \alpha)$. According to Eq. (3·9), we have those oscillator energies $\hbar\omega_+ = \hbar\sqrt{k_+(\alpha)\{1/I + (1 + \cos 2\alpha)/\mu R_e^2\}}$ and $\hbar\omega_- = \hbar\sqrt{k_-(\alpha)\{1/I + (1 - \cos 2\alpha)/\mu R_e^2\}}$, respectively, where $k_+(\alpha)$ and $k_-(\alpha)$ denote spring moduli for respective modes. The moduli are defined by the coefficients of $\Delta\beta_i\Delta\beta_j$ in the harmonic expansion, and have been written in the text as $k_+(\alpha) = k_0 + k_2(\alpha) + k_{\beta}^{12}(\alpha)$ and $k_-(\alpha) = k_0 + k_2(\alpha) - k_{\beta}^{12}(\alpha)$, respectively, where k_0 is a constant, and $k_2(\alpha)$ and $k_{\beta}^{12}(\alpha)$ consist of $\cos(2m\alpha)$ series with $m = \text{even}$ and $m = \text{odd}$, respectively. Since $\cos 2(\alpha + \pi/2) = -\cos 2\alpha$ and this is also the case in $k_{\beta}^{12}(\alpha)$, i.e., $k_{\beta}^{12}(\alpha + \pi/2) = -k_{\beta}^{12}(\alpha)$, we have relations $\hbar\omega_+(\alpha + \pi/2) = \hbar\omega_-(\alpha)$ and $\hbar\omega_-(\alpha + \pi/2) = \hbar\omega_+(\alpha)$. Thus the oscillator functions $\varphi_{n_+}^+(\beta_+, \alpha)$ and $\varphi_{n_-}^-(\beta_-, \alpha)$ also follow the same relations, such as

$$\varphi_{n'}^+(\beta, \alpha) = \varphi_{n'}^-(\beta, \alpha + \pi/2) = \varphi_{n'}^+(\beta, \alpha + \pi), \quad (\text{B} \cdot 7)$$

where the variable β denotes β_+ or β_- . As for the transformation on $\Delta\beta_i$, the operator \mathcal{I}_i is the inversion by the definition, and so we have $\mathcal{I}_1 : (\theta_3, \alpha, \beta_+, \beta_-) \rightarrow (\theta_3 + \pi/2, \alpha + \pi/2, -\beta_-, -\beta_+)$ and $\mathcal{I}_2 : (\theta_3, \alpha, \beta_+, \beta_-) \rightarrow (\theta_3 + \pi/2, \alpha - \pi/2, \beta_-, \beta_+)$. By utilizing the above relations, we perform symmetrization of the basis wave function about \mathcal{I}_i . Starting with the wave function $D_{MK}^J(\theta_i)\chi_K(R, \alpha, \beta_1, \beta_2)$ with Eq. (B·5) for $\chi_K(R, \alpha, \beta_1, \beta_2)$, we obtain

$$\begin{aligned} \Psi_{\lambda} &\equiv (1 + \mathcal{I}_1)(1 + \mathcal{I}_2) \cdot D_{MK}^J(\theta_i) f_n(R) \phi_K(\alpha) \varphi_{n_+}^+(\beta_+, \alpha) \varphi_{n_-}^-(\beta_-, \alpha) \\ &= D_{MK}^J(\theta_i) f_n(R) \{1 + (-1)^{n_+ + n_- - K}\} h_{K n_+ n_-}(\alpha, \beta_+, \beta_-), \end{aligned} \quad (\text{B} \cdot 8)$$

with

$$\begin{aligned} h_{K n_+ n_-}(\alpha, \beta_+, \beta_-) &\equiv \phi_K(\alpha) \varphi_{n_+}^+(\beta_+, \alpha) \varphi_{n_-}^-(\beta_-, \alpha) \\ &\quad + (-i)^K \phi_K(\alpha + \pi/2) \varphi_{n_-}^+(\beta_+, \alpha) \varphi_{n_+}^-(\beta_-, \alpha). \end{aligned} \quad (\text{B} \cdot 9)$$

From the phase in the braces of Eq. (B·8), we obtain the selection rule for β -mode quanta as

$$(-1)^{n_+ + n_-} = (-1)^K. \quad (\text{B} \cdot 10)$$

Note that the second term of the r.h.s. of Eq. (B·9) originates from \mathcal{I}_1 and \mathcal{I}_2 , with n_+ and n_- exchanged.

Subsequently, we perform boson symmetrization and parity-projection by operating $\frac{1}{2}(1 + \mathcal{P}_{12})$ and $\frac{1}{2}\{1 + (-1)^p \mathcal{P}\}$ to Ψ_λ . We obtain the symmetrized wave functions as follows:

$$\begin{aligned} \Psi_\lambda \sim & D_{MK}^J(\theta_i) f_n(R) \left[h_{Kn_+n_-}(\alpha, \beta_+, \beta_-) + (-1)^{p+K} h_{Kn_+n_-}(-\alpha, -\beta_+, \beta_-) \right] \\ & + (-1)^{p+J-K} D_{M,-K}^J(\theta_i) f_n(R) \\ & \times \left[h_{-Kn_+n_-}^*(-\alpha, \beta_+, \beta_-) + (-1)^{p+K} h_{-Kn_+n_-}^*(\alpha, -\beta_+, \beta_-) \right]. \quad (\text{B}\cdot 11) \end{aligned}$$

Note that as the \mathcal{P}_{12} - (or \mathcal{P} -) operation gives $-K$ for the total rotation, we set $-K$ in Eq. (B·11) for $h_{Kn_+n_-}(\alpha, \beta_+, \beta_-)$ -functions consistently, as follows. Since Eq. (B·6) indicates the sign for the cycle for $|K|$, we define as $\phi_{-K}(\alpha) = \phi_K(\alpha)$. With the real functions $\phi_K(\alpha)$, the effects $-K$ in $h_{Kn_+n_-}(\alpha, \beta_+, \beta_-)$ -functions appear only in the phase $(-i)^K$ of the second terms of the r.h.s. of Eq. (B·9) for $K = \text{odd}$ as complex conjugate. We further reduce $h_{Kn_+n_-}(\alpha, \beta_+, \beta_-)$ in Eq. (B·11) with the arguments $-\alpha$ and/or $-\beta_+$. Since the reduced potential in Eq. (3·10) has reflection symmetries at $\alpha = 0$ and $\alpha = \pi/2$, we are able to classify $\phi_K(\alpha)$ by parities with respect to those points, i.e.,

$$\begin{aligned} \phi_K(-\alpha) &= \pi_{\alpha=0} \cdot \phi_K(\alpha), \\ \phi_K(\pi/2 - \alpha) &= \pi_{\alpha=\pi/2} \cdot \phi_K(\pi/2 + \alpha), \end{aligned} \quad (\text{B}\cdot 12)$$

where $\pi_{\alpha=0}$ and $\pi_{\alpha=\pi/2}$ denote the parities with respect to the reflection points, respectively. Note that a relation $\pi_{\alpha=\pi/2} = (-1)^K \pi_{\alpha=0}$ is known because of $\phi_K(\alpha + \pi) = (-1)^K \phi_K(\alpha)$ by Eq. (B·6). Due to $\hbar\omega(-\alpha) = \hbar\omega(\alpha)$ for each β_+ - or β_- -mode, we also know $\varphi_{n'}^+(\beta, -\alpha) = \varphi_{n'}^+(\beta, \alpha)$ and $\varphi_{n'}^-(\beta, -\alpha) = \varphi_{n'}^-(\beta, \alpha)$. By applying Eq. (B·12) to $h_{Kn_+n_-}(\alpha, \beta_+, \beta_-)$ of Eq. (B·9), we rewrite the internal wave functions in Eq. (B·11). For the first line, for example, we obtain

$$\begin{aligned} & h_{Kn_+n_-}(\alpha, \beta_+, \beta_-) + (-1)^{p+K} h_{Kn_+n_-}(-\alpha, -\beta_+, \beta_-) \\ &= \{1 + \pi_{\alpha=0} \cdot (-1)^{p+n_-}\} \left\{ \phi_K(\alpha) \varphi_{n_+}^+(\beta_+, \alpha) \varphi_{n_-}^-(\beta_-, \alpha) \right. \\ & \quad \left. + (-i)^K \phi_K(\alpha + \pi/2) \varphi_{n_-}^+(\beta_+, \alpha) \varphi_{n_+}^-(\beta_-, \alpha) \right\}, \quad (\text{B}\cdot 13) \end{aligned}$$

where the rule Eq. (B·10), $(-1)^K = (-1)^{n_++n_-}$ is used. Hence, relations are obtained as $\pi_{\alpha=0} \cdot (-1)^{p+n_-} = 1$, and for even parity states we have

$$\begin{aligned} \pi_{\alpha=0} &= (-1)^{n_-}, \\ \pi_{\alpha=\pi/2} &= (-1)^{n_+}, \end{aligned} \quad (\text{B}\cdot 14)$$

which specify parities of α -mode in connection with the β -mode quanta. Under the parity selection rule in the α -motion in Eq. (B·14), we can rewrite the functions of Eq. (B·13) into $h_{Kn_+n_-}(\alpha, \beta_+, \beta_-)$. Thus, the final form of the total wave function with the symmetries is as follows:

$$\begin{aligned} \Psi_\lambda \sim & D_{MK}^J(\theta_i) f_n(R) h_{Kn_+n_-}(\alpha, \beta_+, \beta_-) \\ & + (-1)^{J+n_+} D_{M,-K}^J(\theta_i) f_n(R) h_{-Kn_+n_-}(\alpha, \beta_+, \beta_-), \end{aligned} \quad (\text{B}\cdot 15)$$

with the definition of $h_{Kn_+n_-}(\alpha, \beta_+, \beta_-)$ in Eq. (B·9) and with the selection rules given in Eq. (B·10) and Eq. (B·14).

Restrictions on quantum numbers

As a summary, we have selection rules given in Eqs. (B·10) and (B·14), some conditions for the wave functions such as given in Eq. (B·7) and the total wave function given in Eq. (B·15) with Eq. (B·9). In the following, we give some practical selection rules reduced from those relations.

Due to the cyclic condition $\phi_K(\alpha + \pi) = (-1)^K \phi_K(\alpha)$, if we expand $\phi_K(\alpha)$ with periodic functions such as $\cos \nu\alpha$ or $\sin \nu\alpha$, we have a general restriction for rotational quantum numbers $(K \pm \nu) = 2m$, m being an integer. And then, with a specified K , one of the two parities of Eq. (B·14) is enough for specifying $\phi_K(\alpha)$ to be cosine type or sine one, the other selection rule being automatically fulfilled. Because of the symmetry of each constituent nucleus under space inversion, n_+ can be taken to be larger than or equal to n_- . In the case that n_+ is equal to n_- , we have $K = \text{even}$ from $(-1)^{n_++n_-} = (-1)^K$ of Eq. (B·10). And Eq. (B·9) turns out to be $\{\phi_K(\alpha) + (-i)^K \phi_K(\alpha + \pi/2)\} \varphi_{n'}^+(\beta_+, \alpha) \varphi_{n'}^-(\beta_-, \alpha)$, which suggests $(K \pm \nu) = 4m$. (See also Eq. (C·2) for K -, ν -rules.) As for $K = 0$, we obtain the phase rule $(-1)^{J+n_+} = 1$ from Eq. (B·15), i.e., $n_+ = \text{even}$ and $n_- = \text{even}$ for $J = \text{even}$. With $K = \nu = 0$, the state has no α -dependence and hence the second term of Eq. (B·11) become to be the same as the first term, which gives the phase rule $(-1)^{p+J} = 1$, i.e., $J = \text{even}$ for the positive-parity states and $J = \text{odd}$ for the negative-parity states, respectively.

Appendix C

— Explicit Expressions of Wave functions for the Normal Modes —

In the present Appendix, we give some examples of explicit expressions for the wave functions. As is shown in Appendix B, the internal wave functions are approximately a product of $f_n(R)$, $\phi_K(\alpha)$, $\varphi_{n_+}^+(\beta_+, \alpha)$ and $\varphi_{n_-}^-(\beta_-, \alpha)$, which are essentially oscillator wave functions except for $\phi_K(\alpha)$. The property of α -motion may be rotational, or may be vibrational, depending on the strength of the reduced potential which confines the alpha-degree of freedom. Note that the reduced potential is determined by the interaction between two nuclear surfaces as well as by quantum states of the other degrees of freedom. Especially in the molecular ground state, where the additional potentials from the normal-mode motions such as the butterfly mode is weak, the property of $\phi_K(\alpha)$ is determined by the interaction. The confinement potential obtained from the folding model is weak as is shown in §3, but its reality is not confirmed yet. Hence we present both types for $\phi_K(\alpha)$ functions, i.e., cosine and sine series as well as gaussian functions. First we take up the rotational type and adopt cosine series for $\phi_K(\alpha)$, assuming $K, \nu = \text{even}$ and $n_+, n_- = \text{even}$. Note that $e^{i\nu\alpha}$ may be convenient for describing $h_{Kn_+n_-}(\alpha, \beta_+, \beta_-)$ in Eq. (B·9), but it does not fulfill Eqs. (B·12) and (B·14). Note also that for $K = \text{odd}$, $h_{Kn_+n_-}(\alpha, \beta_+, \beta_-)$ includes both cosine and sine functions due to the shift by $\pi/2$ in $\phi_K(\alpha)$.

Now we write down the total wave function according to Eqs. (B·9) and (B·15).

For positive-parity states with $K = \text{even}$ and $n_+ = \text{even}$ ($n_- = \text{even}, \pi_{\alpha=\pi/2} = \pi_{\alpha=0} = 1$), by applying $\cos \nu(\alpha + \pi/2) = (-1)^{\nu/2} \cos \nu\alpha$ for $\phi_K(\alpha + \pi/2)$, we have

$$\Psi_\lambda \sim \left[D_{MK}^J(\theta_i) + (-1)^J D_{M,-K}^J(\theta_i) \right] f_n(R) h_{Kn_+n_-}(\alpha, \beta_+, \beta_-), \quad (\text{C}\cdot 1)$$

with

$$h_{Kn_+n_-}(\alpha, \beta_+, \beta_-) \equiv \sum_{\nu=\text{even}} C_\nu \cos \nu\alpha \left\{ \varphi_{n_+}^+(\beta_+, \alpha) \varphi_{n_-}^-(\beta_-, \alpha) + (-1)^{\frac{K+\nu}{2}} \varphi_{n_-}^+(\beta_+, \alpha) \varphi_{n_+}^-(\beta_-, \alpha) \right\}. \quad (\text{C}\cdot 2)$$

If we take a single value of ν , the α -motion is, of course, rotational. The quantum state $(n, n_+, n_-, K, \nu) = (0, 0, 0, 0, 0)$ corresponds to the molecular ground state. Actually the solutions obtained in §3 is close to that with $\nu = 0$. For $K = 0$, the next rotational state is with $\nu = 4$, namely, the *twisting rotational mode*. The explicit functions for $h_{Kn_+n_-}(\alpha, \beta_+, \beta_-)$ of those states are given as

$$\begin{aligned} \nu = 0 : \quad h_{000}(\alpha, \beta_+, \beta_-) &= \sqrt{\frac{1}{\pi}} \varphi_0^+(\beta_+, \alpha) \varphi_0^-(\beta_-, \alpha), \\ \nu = 4 : \quad h_{000}(\alpha, \beta_+, \beta_-) &= \sqrt{\frac{2}{\pi}} \cos 4\alpha \varphi_0^+(\beta_+, \alpha) \varphi_0^-(\beta_-, \alpha). \end{aligned} \quad (\text{C}\cdot 3)$$

Due to the weak α -dependence of the folding potential, solutions receive small mixings over ν . The molecular ground state has the $\nu = 4$ component about 3% in the probability, as well as the $\nu = 0$ component in the $\nu = 4$ excited state. Those coefficients C_ν 's are adopted for the calculations of the partial decay widths and the angular correlations, with the approximation of the constant vibrational quanta for \hbar_{β_+} and \hbar_{β_-} ($\hbar_{\beta_+} = \hbar_{\beta_-}$), the value of which is taken to be 4MeV. As for the relative motion, it is completely separated from the $(\alpha, \beta_+, \beta_-)$ -degrees of freedom, and it is described by oscillator wave function $f_n(R)$ with the center at the equilibrium distance R_e . According to the experimental resonance energy $E_{\text{cm}} = 55.8\text{MeV}$ for $J = 38$, the molecular ground state with $n = 0$ is a suitable assignment as the theoretical eigenenergy is 51.5MeV. With $n = 1$, the radially-excited state appears at higher than experimental energy, and it may not be observed in experiments, because of the broad decay widths expected. On the other hand, there is a possibility that a stronger interaction appears due to induced deformations, which give rise to lowering the eigenenergy of the radially-excited state to 55.8MeV. Note that characteristics of probability distributions among the decay channels receive no effect from the choice of the radial motion with given n , which is completely separated from the angle degrees of freedom. Only the magnitudes of the partial decay widths commonly become larger as we take a higher n -value.

If we coherently sum over ν in Eq. (C·2), the α -motion can have a localized property such as a zero-point oscillation. For example, for simplicity, we take up $n_+ = n_- = 0$, and then the selection rule for K and ν is $K \pm \nu = 4m$ with m being an integer, because two terms in the braces of the r.h.s. of Eq. (C·2) must have the

same sign. We can write simply as

$$h_{K00}(\alpha, \beta_+, \beta_-) = \sum_{K+\nu=4m} C_\nu \cos \nu \alpha \varphi_0^+(\beta_+, \alpha) \varphi_0^-(\beta_-, \alpha). \quad (\text{C}\cdot 4)$$

Now, if we adopt gaussian type coefficients for C_ν by

$$C_\nu = \frac{4}{1 + \delta_{\nu 0}} \left(\frac{1}{a\pi^3} \right)^{1/4} \exp \left(-\frac{\nu^2}{2a} \right), \quad (\text{C}\cdot 5)$$

we obtain localized α -motion such as

$$\begin{aligned} \text{gaussian : } h_{K00}(\alpha, \beta_+, \beta_-) = & \left(\frac{a}{4\pi} \right)^{1/4} \left[\exp \left(-\frac{a}{2} \alpha^2 \right) + (-1)^{K/2} \exp \left\{ -\frac{a}{2} \left(\alpha - \frac{\pi}{2} \right)^2 \right\} \right] \\ & \times \varphi_0^+(\beta_+, \alpha) \varphi_0^-(\beta_-, \alpha), \end{aligned} \quad (\text{C}\cdot 6)$$

where the normalization constant is given for the case with no substantial overlapping between two terms in the square bracket on the r.h.s. of Eq. (C·6). Note that due to the application of the selection rule $K \pm \nu = 4m$ on $\cos \nu \alpha$, the resultant α -function (the second line of Eq. (C·6)) is periodic with period π , and especially for $K = 4n$ the function is with period $\pi/2$. Our expression for the variable α in Eq. (C·6) is given for the region $-\pi/4 \leq \alpha < 3\pi/4$, so that the next gaussian peak at $\alpha = \pi$ can be omitted.

The normal modes for the β_+ - and β_- -motions are named as *butterfly* and *anti-butterfly modes*, respectively, the quantum numbers of which are (n_+, n_-) . Due to the selection rule $(-1)^{n_+ + n_-} = (-1)^K$, the lowest butterfly and anti-butterfly states with $K = 0$ appear with $(n_+, n_-) = (2, 0)$ and $(0, 2)$, respectively. The physical butterfly motion corresponds to the configuration displayed in Fig. 2, where the motion of the axis z_2'' is confined around downside with $\alpha_2 \sim \pi$ and the vibrational motions with $\Delta\beta_1 \sim \Delta\beta_2$, for example, with the quanta $(2, 0)$. When the configuration described with variables α_i and $\Delta\beta_i$ is transformed by $\mathcal{I}_2 : (\alpha_2, \beta_2) \rightarrow (\alpha_2 + \pi, \pi - \beta_2)$ in Eq. (B·3), (β_+, β_-) is transformed into (β_-, β_+) , which means that the physical butterfly motion is also described with configurations with the motion of the axis z_2'' confined around upside with $\alpha_2 \sim 0$ and the vibrational motions with $\Delta\beta_1 \sim -\Delta\beta_2$, with the quanta $(0, 2)$ as the example. Those symmetric terms for (n_+, n_-) exchange are described in Eq. (B·9) and Eq. (C·2), where wave functions for the lowest butterfly state $h_{K20}(\alpha, \beta_+, \beta_-)$ consist with one term with $(2, 0)$ of $\alpha \sim \pi/2$ and another term with $(0, 2)$ of $\alpha \sim 0$; for example, for butterfly,

$$\begin{aligned} & \left(\frac{a}{4\pi} \right)^{1/4} \left[(-1)^{K/2} \exp \left\{ -\frac{a}{2} \left(\alpha - \frac{\pi}{2} \right)^2 \right\} \varphi_2^+(\beta_+) \varphi_0^-(\beta_-) \right. \\ & \quad \left. + \exp \left(-\frac{a}{2} \alpha^2 \right) \varphi_0^+(\beta_+) \varphi_2^-(\beta_-) \right], \end{aligned} \quad (\text{C}\cdot 7)$$

with a zero-point oscillation assumed for the α -degree, while for anti-butterfly,

$$\begin{aligned} & \left(\frac{a}{4\pi} \right)^{1/4} \left[(-1)^{K/2} \exp \left\{ -\frac{a}{2} \left(\alpha - \frac{\pi}{2} \right)^2 \right\} \varphi_0^+(\beta_+) \varphi_2^-(\beta_-) \right. \\ & \quad \left. + \exp \left(-\frac{a}{2} \alpha^2 \right) \varphi_2^+(\beta_+) \varphi_0^-(\beta_-) \right]. \end{aligned} \quad (\text{C}\cdot 8)$$

We have solved the Schrödinger equation for the α -degree in §3, where we worked with the reduced potential for the butterfly quanta $(2, 0)$ and obtained the solutions $\phi_K(\alpha)$. A butterfly state appears with the lowest energy with a localization around $\alpha = \pi/2$ as is seen in Fig. 7. The motion for the α -degree of an anti-butterfly state which corresponds to the quanta $(2, 0)$, i.e., $\phi_K(\alpha)$ for the second term of Eq. (C-8) is obtained with an excitation. In order to calculate the partial widths and the angular correlations for the butterfly states, we use a simple but a typical expression, in which $\phi_K(\alpha)$ are described with dominant two coefficients C_0 and C_2 in Eq. (C-2). Furthermore to obtain a typical expression, we impose a symmetry between the α -motions in the butterfly and anti-butterfly states. Then we have the expression for the *butterfly* state with $K = \text{even}$ as

$$h_{K20}(\alpha, \beta_+, \beta_-) = \frac{1}{2\sqrt{\pi}} \left[(-1)^{K/2} (1 - \sqrt{2} \cos 2\alpha) \varphi_2(\beta_+) \varphi_0(\beta_-) + (1 + \sqrt{2} \cos 2\alpha) \varphi_0(\beta_+) \varphi_2(\beta_-) \right], \quad (\text{C-9})$$

where the oscillator $\varphi_n^\pm(\beta_\pm, \alpha)$ are also simplified to be independent upon α with an averaged oscillator energy. The corresponding pair of the *anti-butterfly* state is given by

$$h_{K02}(\alpha, \beta_+, \beta_-) = \frac{1}{2\sqrt{\pi}} \left[(-1)^{K/2} (1 - \sqrt{2} \cos 2\alpha) \varphi_0(\beta_+) \varphi_2(\beta_-) + (1 + \sqrt{2} \cos 2\alpha) \varphi_2(\beta_+) \varphi_0(\beta_-) \right]. \quad (\text{C-10})$$

As the dynamical solutions for the α -motions in the reduced potential with the quanta $(2, 0)$, $\phi_K(\alpha)$ are simplified to be $(1 - \sqrt{2} \cos 2\alpha)$ for the butterfly mode, while they are $(1 + \sqrt{2} \cos 2\alpha)$ for the anti-butterfly mode. Note that the results of our dynamical calculations with the reduced potential are rather close to those typical expressions.

Wobbling motion (K -mixed states)

Following the discussion on K -mixed states in §4.1, we define a wave function for the wobbling motion. The mixing weights are given by a gaussian function of K , by which we superpose $D_{MK}^J(\theta_i)$ such as

$$\sum_K \tilde{C}_K \sqrt{\frac{2J+1}{8\pi^2}} D_{MK}^J(\theta_i) = \sqrt{\frac{2J+1}{4\pi}} e^{iM\theta_1} d_{MK}^J(\theta_2) \sum_K \tilde{C}_K \frac{e^{iK\theta_3}}{\sqrt{2\pi}}, \quad (\text{C-11})$$

with

$$\tilde{C}_K = \begin{cases} \sqrt{\frac{2}{b\sqrt{\pi}}} \exp \left[-\frac{1}{2} \left(\frac{K}{b} \right)^2 \right] & \text{for } K = \text{even} \\ 0 & \text{for } K = \text{odd}, \end{cases} \quad (\text{C-12})$$

where $|\Delta K| = 2$ due to the nature of couplings due to the axial asymmetry. The term with $K = 0$ is important for including the components of the elastic scattering. The coherent summation over $\tilde{C}_K e^{iK\theta_3}/\sqrt{2\pi}$ again gives us a gaussian function $W(\theta_3)$ of

period π due to $K = \text{even}$. We obtain, for $0 \leq \theta_3 < 2\pi$,

$$W(\theta_3) = \sqrt{\frac{b}{2\sqrt{\pi}}} \left[\exp \left\{ -\frac{b^2}{2} \theta_3^2 \right\} + \exp \left\{ -\frac{b^2}{2} (\theta_3 - \pi)^2 \right\} + \exp \left\{ -\frac{b^2}{2} (\theta_3 - 2\pi)^2 \right\} \right]. \quad (\text{C}\cdot 13)$$

The wobbling basis function of Eq. (C·11) would be applied with the internal modes $\chi_K(R, \alpha, \beta_+, \beta_-)$ of Eq. (B·5), which receives the transformations \mathcal{I}_i given in Eq. (B·3), and is symmetrized as in Eq. (B·8). When we sum over $D_{MK}^J(\theta_i)$ of different K -values, relative phases of those functions should be chosen properly. The coefficients for the wobbling motion in Eq. (C·11) is given for the axially asymmetric configurations, where the molecular axis with the largest moment of inertia is x' , i.e., $I_{x'} > I_{y'}$, such as for an equator-equator one illustrated in Fig. 8. However the butterfly configuration such as illustrated in Fig. 2 has $I_{x'} < I_{y'}$, because, with $\alpha_1 = 0$ and $\alpha_2 = \pi$, i.e., $\theta_3 = \pi/2$ and $\alpha = -\pi/2$ by definition, the x' -axis moves to the direction of the initial y' -axis. To recover the condition $I_{x'} > I_{y'}$, we need to reset the x' -axis on to the initial direction, which brings additional phases $e^{-i\pi/2} = (-i)^K$ on $D_{MK}^J(\theta_i)$. The expressions in Eqs. (C·6)~(C·10) satisfy this relative phase convention. Of course, we are able to adopt the rotational equation of motion with $I_{x'} < I_{y'}$ in §4.1, to obtain the alternative phase $(-1)^{K/2}$ for the K -bases.

Appendix D

— Moments of Inertia of Dinuclear Systems —

The expression of the inertia tensor of dinuclear systems is already given in Eq. (2·8), which is defined by the configuration referring to the molecular axes. We again write it here, for convenience, i.e.,

$$\mathbf{I}_s = \mathbf{I}_\mu(R) + {}^tR'(\alpha_1\beta_1\gamma_1) \mathbf{I}_1 R'(\alpha_1\beta_1\gamma_1) + {}^tR'(\alpha_2\beta_2\gamma_2) \mathbf{I}_2 R'(\alpha_2\beta_2\gamma_2), \quad (\text{D}\cdot 1)$$

where the first term of the r.h.s. denotes the moments of inertia of two-ion centers, and the second and third terms are individual contributions from the constituent nuclei with rotation matrices $R'(\alpha_i\beta_i\gamma_i)$. The diagonal components I_{11} and I_{22} of the inertia tensor $\mathbf{I}_\mu(R)$ are μR^2 , the others being zero. The inertia tensors of the two constituent nuclei, \mathbf{I}_1 and \mathbf{I}_2 are defined in the coordinate frames of their principal axes. Then, they are diagonal, elements of which are determined by the excitation energies of the members of the ground rotational bands of the constituent nuclei. Except for the relative vector of the two-ion centers, the whole dinuclear configuration is determined by the orientations of the principal axes of the constituent nuclei, due to Euler rotations $\Omega'_i(\alpha_i, \beta_i, \gamma_i) \Omega_M(\theta_1, \theta_2)$. In them, the first rotation $\Omega_M(\theta_1, \theta_2)$ is concerned about the molecular axes, and the second rotation $\Omega'_i(\alpha_i\beta_i\gamma_i)$ is that of each constituent nucleus referring to the molecular axes. Thus the moments of inertia about the molecular axes are obtained with the rotation matrices $R'(\alpha_i\beta_i\gamma_i)$.

We estimate magnitudes of the moments of inertia from the shape of the molecular configuration displayed in Fig. 8. Inserting $\alpha_1 = \alpha_2 = 0$ and $\beta_1 = \beta_2 = \pi/2$, we obtain the diagonal elements of \mathbf{I}_s to be

$$\begin{aligned}
I_x &= \mu R^2 + I_a + I_b, \\
I_y &= \mu R^2 + I_A + I_B, \\
I_z &= I_A + I_B,
\end{aligned}
\tag{D·2}$$

with the nondiagonal elements being zero. I_A etc. denote the moments of inertia of the constituent nuclei, individually in their principal axes, i.e., the diagonal elements (I_1, I_2, I_3) of \mathbf{I}_1 are written as (I_A, I_A, I_a) , and those of \mathbf{I}_2 as (I_B, I_B, I_b) , and their nondiagonal elements are zero. Note that for the states of the ground rotational band of the ^{28}Si nucleus, due to the axial symmetry, $I_1 = I_2$ is assumed and further $I_a = I_b = 0$ is adopted in §2.

The value of the moment of inertia \mathcal{I} for the ^{28}Si ground band, is determined from the excitation energy $E_x = 1.78\text{MeV}$ of the 2_1^+ state of the ^{28}Si nucleus, i.e., by the relation,

$$\frac{\hbar^2}{2\mathcal{I}}I(I+1) = E_x, \tag{D·3}$$

I being the spin value ($I = 2$), and the value of \mathcal{I} is used in the numerical calculations in §3. Note that $I_A = I_B = \mathcal{I}$ is denoted by I in Eq. (2·20).

On the other hand, moments of inertia of rigid bodies have been often investigated in the study of rotational spectra.³⁷⁾ In §4.1, with respect to the nuclear shape of the whole system, we adopt I_a and I_b of nonzero value, where induced deformation is expected. Moments of inertia can be obtained by integrating over nuclear volume, such as

$$I_i = \int_V \rho(\mathbf{r})(r^2 - x_i^2)dV, \tag{D·4}$$

where x_i denote the coordinates in the principal axes, and $\rho(\mathbf{r})$ is a nuclear density distribution. The density profile of ^{28}Si appears in the calculations of the folding potential with DDM3Y force in §2.3, and its parameters are given there. With induced deformation, I_1 is not necessary to be equal to I_2 , but we take the value of $I_1 = I_2$ tentatively, due to the axial symmetry of the density profile. Due to the oblate shape of the density profile, we obtain the vales of $I_1 = I_2 < I_3$, the values of which are (164, 164, 222) in the unit of M_nfm^2 , with M_n being the nucleon mass. Compared with the value of moment of inertia, $70\text{M}_n\text{fm}^2$ estimated by Eq. (D·3), the value $164\text{M}_n\text{fm}^2$ is about two times larger than that, which is well known for rotational spectra of nuclei.³⁷⁾ Since the moments of inertia of rigid body are too large, we renormalize the values of moments of inertia obtained by Eq. (D·4), to be consistent with the excitation energy of the 2_1^+ state of the ^{28}Si nucleus. This means that we multiply a factor 0.42 on the moments of inertia of Eq. (D·4). Thus a value $I_a = I_b = 93\text{M}_n\text{fm}^2$ is adopted, and Eqs. (D·2) give the values for moments of inertia of the whole system. Note that $I_1 = I_2$ is broken with induced deformation of the ^{28}Si nucleus, but we have no information about those changes of the moments of inertia. Hence we adopt the same value $70\text{M}_n\text{fm}^2$ for I_A with the assumption $I_1 = I_2$, as well as for I_B .

As for dinuclear configurations in §4.2, since one of the constituent nuclei is spherical, i.e., $I_2 = 0$ in Eq. (D·1), we obtain the expressions of moments of inertia by simply inserting $I_B = I_b = 0$ into Eq. (D·2). Note that those expressions are tailored for the configurations displayed in Fig. 11(b) and Fig. 12, where I_A and I_a are denoted as I_0 and I_3 , respectively, because of no I_2 . For case 1, $I_a = 0$ is adopted with the axially-symmetric deformation, and for case 2, $I_a \neq 0$ is adopted with the axially-asymmetric one, in which the ratio I_a/I_A can be estimated by Eq. (D·4).

References

- 1) R. R. Betts, *Proc. Intern. Conf. on Nuclear Physics with Heavy Ions, Stony Brook, 1983*, ed. P. Braun-Munzinger (Harwood academic pub., New York, 1984), p. 347.
- 2) R. R. Betts, *Proc. Second Intern. Conf. on Nucleus-Nucleus Collisions, Visby, 1985*, eds. H.Å. Gustafsson et al.: Nucl. Phys. **A447** (1986), 257.
- 3) R. R. Betts, S. B. DiCenzo and J. F. Petersen, Phys. Rev. Lett. **43** (1979), 253.
- 4) R. R. Betts, S. B. DiCenzo and J. F. Petersen, Phys. Lett. **100B** (1981), 117.
- 5) R. R. Betts, B. B. Back and B. G. Glagola, Phys. Rev. Lett. **47** (1981), 23.
- 6) S. Saini and R. R. Betts, Phys. Rev. C **29** (1984), 1769.
- 7) R. W. Zurmühle et al., Phys. Lett. **129B** (1983), 384.
- 8) S. Saini et al., Phys. Lett. B **185** (1987), 316.
- 9) C. Beck, R. Nouicer, et al., Phys. Rev. C **63** (2000), 014607.
- 10) Y. Abe, Y. Kondō and T. Matsuse, Prog. Theor. Phys. Suppl. No. 68 (1980), 303, and references therein.
- 11) M. Faber and M. Płoszajczak, Physica Scripta **24** (1981), 189.
S. Åberg, *Proc. Work Shop on Nuclear Structure and Heavy-ion Reaction Dynamics, Notre Dame, 1990*, eds. R.R. Betts and J.J. Kolata (Inst. Phys. Conf. Ser. No 109), p. 143.
- 12) T. Bengtsson et al., Preprint Lund-MPh-84/01 (1984), and also in Ref. 1).
- 13) R. K. Gupta et al., J. Phys. G **35** (2008), 075106.
- 14) J. Darai et al., Phys. Rev. C **84** (2011), 024302.
- 15) R. Maass and W. Scheid, Phys. Lett. B **202** (1988), 26.
- 16) R. A. Broglia, C. H. Dasso, H. Esbensen and A. Winther, Nucl. Phys. **A349** (1980), 496.
- 17) E. Uegaki and Y. Abe, Phys. Lett. B **231** (1989), 28.
- 18) E. Uegaki and Y. Abe, Prog. Theor. Phys. **90** (1993), 615.
- 19) E. Uegaki and Y. Abe, Phys. Lett. B **340** (1994), 143.
- 20) E. Uegaki, Prog. Theor. Phys. Suppl. No. 132 (1998), 135.
- 21) S. W. Ødegård *et al.*, Phys. Rev. Lett. **86** (2001), 5866.
Y. R. Shimizu, M. Matsuzaki and K. Matsuyanagi, Phys. Rev. C **72** (2005), 014306.
- 22) R. Nouicer, C. Beck, et al., Phys. Rev. C **60** (1999), 041303(R).
- 23) R. Bass, *Nuclear Reactions with Heavy Ions* (Springer-Verlag, Berlin, 1980), p. 259.
- 24) E. Uegaki and Y. Abe, Prog. Theor. Phys. **127** (2012), 877.
- 25) For example, N. Olsson, E. Ramström and B. Trostell, Nucl. Phys. **A513** (1990), 205, and references therein.
- 26) A. S. Davydov and B. F. Fillipov, Nucl. Phys. **8** (1958), 237.
- 27) J. Blocki, J. Randrup, J. Swiatecki and C. F. Tsang, Ann. of Phys. **105** (1977), 427.
- 28) M. El-Azab Farid and G. R. Satchler, Nucl. Phys. **A438** (1985), 525.
- 29) G. R. Satchler and W. G. Love, Phys. Rep. **55** (1979), 183.
- 30) C. R. Howell et al., Phys. Rev. C **38** (1988), 1552.
- 31) P. M. Endt, Nucl. Phys. **A521** (1990), 1.
- 32) A. Bohr and B. R. Mottelson, *Nuclear Structure vol. I* (Benjamin, New York, 1969), p. 158.
- 33) T. Takatsuka, Prog. Theor. Phys. **73** (1985), 1043.
- 34) J. P. Blaizot, Phys. Rep. **64** (1980), 171.
- 35) A. Bohr and B. R. Mottelson, *Nuclear Structure vol. II* (Benjamin, Massachusetts, 1975), p. 175.
- 36) M.-D. Salsac et al., Nucl. Phys. A **801** (2008), 1.
- 37) For example, in Ref. 35), p. 74.